

# Fuzzy-logic indicators for riverbed de-clogging suggest ecological benefits of large wood

Sebastian Schwindt<sup>a,\*</sup>, Beatriz Negreiros<sup>a</sup>, Maria Ponce<sup>a</sup>, Isabella Schalko<sup>b,c</sup>, Simone Lassar<sup>b,d</sup>, Ricardo Barros<sup>e</sup>, Stefan Haun<sup>a</sup>

<sup>a</sup> Institute for Modelling Hydraulic and Environmental Systems, University of Stuttgart, Stuttgart, Germany

<sup>b</sup> Department of Civil and Environmental Engineering, Massachusetts Institute of Technology, Cambridge, MA, USA

<sup>c</sup> Institute of Fluid Dynamics, Department of Mechanical and Process Engineering, ETH Zurich, Zurich, Switzerland

<sup>d</sup> Natel Energy, Alameda, CA, USA

<sup>e</sup> Institute for Water and River Basin Management, Karlsruhe Institute of Technology, Karlsruhe, Germany

## ARTICLE INFO

### Keywords:

MultiPAC  
Fine sediment  
Hyporheic exchange  
Colmation  
Ecohydraulics

## ABSTRACT

Rivers provide dynamic habitats with ecological niches, particularly in their mobile sand, gravel, and cobble riverbed patches that create an active hyporheic zone. Natural or artificial deposition of fine sediment may clog the porous matrix of the hyporheic zone, impairing exchange processes between the subsurface and surface water. Clogging reduces the permeability of the sediment matrix, thus degrading the ecological functionality of the hyporheic zone. Once clogged, the ecological functions may be recovered through active stream restoration, which requires considerate site assessment. To this end, clogging is typically assessed by expert opinion of substrate characteristics including grain size characteristics, porosity, hydraulic conductivity, and interstitial oxygen content. To overcome limitations of expert assessment, such as subjectivity expressed in noisy decision-making, this study introduces a novel fuzzy-logic method based on physically sound rules. The method provides quantitative indicators for clogging and declogging to evaluate the effectiveness of stream restoration. We applied the fuzzy-logic method to test whether the placement of large wood, a common restoration practice, can locally prevent or reduce clogging. Two measurement series from before and after a morphologically effective flood suggested that large wood placements perpendicular to the flow generate elevated amounts of declogging. The tested logs caused a greater amount of declogging within their region of influence than observed at a reference point. The effect was stronger for a log emergent at baseflow. The declogging assessment showed that the novel fuzzy-logic indicators can reasonably overcome subjective judgment by accounting for multi-variate quantitative changes rather than individual parameter trends.

## 1. Introduction

Many restoration techniques exist for improving the ecological status of river environments, but the scientific basis of river restoration still requires substantial enrichment (Pasternack, 2020). Specifically, the implementation of restoration actions is a major challenge because of high system complexity and uncertain definitions of success (Allan and Castillo, 2007). Even in near-natural rivers, restoration efforts are performed to address functional shortcomings, such as missing vertical connectivity between surface and subsurface flows in the hyporheic zone (the region where surface water and groundwater mix) (Boulton, 2007). For instance, bedload transport discontinuity may cause a surplus

of fine sediment, which infiltrates into the grain matrix of cobble-gravel-bed rivers (Cunningham et al., 1987; Einstein, 1968). This process, called riverbed clogging, siltation, colmation, or colmatation (Blaschke et al., 2003; Dubuis and De Cesare, 2023; Schälchli, 1992), occurs when fine sediment or organic matter congests the porous space of the sediment matrix of a primarily coarse riverbed (Battin and Sengschmitt, 1999; Brunke and Gonser, 1997; Einstein, 1970; Wood and Armitage, 1997). The resulting reduction in available pore space also involves reduced hydraulic conductivity of the riverbed (Blaschke et al., 2003; Lisle, 1989; Schaelchli, 1992). Although clogging may occur naturally in response to hydrological conditions, anthropogenic impacts have considerably intensified clogging (Wharton et al., 2017). The disruption

\* Corresponding author.

E-mail addresses: [sebastian.schwindt@iws.uni-stuttgart.de](mailto:sebastian.schwindt@iws.uni-stuttgart.de) (S. Schwindt), [ricardovbarros@live.com](mailto:ricardovbarros@live.com) (R. Barros).

<https://doi.org/10.1016/j.ecolind.2023.111045>

Received 7 July 2023; Received in revised form 1 September 2023; Accepted 2 October 2023

Available online 5 October 2023

1470-160X/© 2023 The Authors. Published by Elsevier Ltd. This is an open access article under the CC BY license (<http://creativecommons.org/licenses/by/4.0/>).

of vertical linkages caused by clogging also affects the chemo-physical habitat quality of river ecosystems. For example, the substrate consolidation caused by clogging makes it difficult or impossible for gravel-spawning fish to dig redds for their eggs (Chapman, 1988; Moring, 1982). In addition, clogging hinders the flow of oxygen-rich surface water into the riverbed, thus reducing the available amount of oxygen in the interstitial, which lowers both survival rates in the redds and species abundance of macroinvertebrates (Eriksen, 1968; Grygoruk et al., 2021; Harrod and Theurer, 2002; Jones et al., 2012; Wood and Armitage, 1997).

The first step in addressing clogging is its quantification. Approaches to assessing clogging *in-situ* involve, for instance, monitoring fine sediment infiltration with sediment traps or catch trays (Fletcher et al., 1995; Franssen et al., 2014; Harper et al., 2017), grain size analysis (Gibson et al., 2009; Nagel et al., 2020; Petts et al., 1989), expert-based visual mapping of clogged surfaces (Schaelchli, 2002), oxygenation levels of the riverbed (Marmonier et al., 2004), or electrical resistivity tomography (Ulrich et al., 2015). In addition, tools like the Kolmometer (Zumbroich and Hahn, 2018) or Penetrometer (Mohammadi et al., 2008) provide indirect measures of flow resistance and compactness of the riverbed. Also, quantitative, single-parameter methods have been proposed to estimate a degree of clogging (Datry et al., 2015). Beyond grain characteristics and oxygen saturation, the hydraulic conductivity of soils also is a crucial parameter for characterizing clogging (Descloux et al., 2010). The hydraulic conductivity can be approximated by means of tracer tests (Packman et al., 2004) or back-calculated from so-called slurp test (Seitz, 2020). While clogging is a function of physical, biological, and chemical factors (Sennatt et al., 2006), there is no standardized quantitative approach to assess clogging based on multiple parameters in spatial and temporal scales (Dubuis and De Cesare, 2023). Thus, a holistic quantification of clogging embraces multiple parameters, which can be measured with the so-called Multi-Parameter Approach to assess Clogging (MultiPAC) (Negreiros et al., 2023a; Seitz, 2020). This study builds on MultiPAC and explains the involved devices in detail to measure a set of five individual parameters, notably the fine sediment fraction, a ratio characterizing the width of the grain size distribution, porosity, hydraulic conductivity, and interstitial oxygen content. Each of the parameters provides information on clogging, but in some cases, individual parameters may yield conflicting conclusions regarding the state of clogging. For instance, a fine-sediment riverbed may still experience high oxygen saturation while the porosity is low. To harmonize measured trends in multiple parameters, we asked in this study: *how can riverbed clogging be holistically and objectively assessed based on multiple physio-chemical substrate parameters?* To answer this question, we developed a novel fuzzy-logic method that we used to test a hypothesis for effectively mitigating clogging through local restoration efforts.

Restoration and habitat improvement efforts generally aim at counteracting anthropogenic habitat degradation, including clogging. However, river section-wide measures with a large spatial footprint, such as gravel augmentation (Bunte, 2004) or environmental flow releases (Acreman et al., 2014), require years-long, complex, and multi-disciplinary planning. In contrast, locally effective restoration actions at the scale of morphological units, that is, 1 to 10 times the channel width (Pasternack and Wyrick, 2017), can be easier implemented (Albert et al., 2021). One option for restoration at the morphological-unit scale is the placement of locally sourced, large wood (LW), defined as logs with a diameter  $\geq 0.10$  m and a length  $\geq 1$  m (Keller and Swanson, 1979). LW placement or engineered logjams correspond to a nature-based solution (NBS) aiming to create heterogeneous flow conditions and local morphological structures (Grabowski et al., 2019; Wohl et al., 2015). At the tips of an LW placement, the flow velocity and bed shear stress are elevated. Similar to a bluff body, a wake region with reduced flow velocity and elevated turbulence is created downstream of a LW placement (Schalko et al., 2021). This wake region can provide valuable habitat for fish species (Fausch, 1993; Roni et al., 2015; Schalko et al., 2021; Smith

et al., 2014). For instance, LW was found to aid Pacific salmon in spawning their eggs (Senter and Pasternack, 2011) and provide habitat for juvenile coho salmon (Tullos and Walter, 2015). We hypothesized that LW placements can promote declogging, particularly at flood stages, due to an increase in hyporheic exchange (Doughty et al., 2020; Sawyer et al., 2011), governed by the elevated upstream water depth, and increased turbulence at the tips and in the wake. Therefore, we installed two logs with similar diameters at different riverbed depths in a near-natural fish pass, such that one was submerged and one emergent at baseflow depth. After the installation, we triggered an artificial, morphologically effective flood (Leopold and Wolman, 1957; Wolman and Leopold, 1957; Wolman and Miller, 1960). To test the hypothesis with the new fuzzy-logic method, parameters characterizing clogging were measured with MultiPAC before and after the artificial flood in the vicinity of the LW placements to calculate a newly developed indicator of a normalized degree of clogging and to test the relevance of LW placement as a tool for targeted river restoration to reduce clogging.

## 2. Methods

### 2.1. *In-situ* assessment of riverbed clogging with MultiPAC

#### 2.1.1. MultiPAC instrumentation

MultiPAC embraces measurements of hydraulic conductivity, dissolved oxygen, and freeze core samples taken within a maximum distance of 0.5 m between two different types of standpipes (Fig. 1). Since a freeze core destroys the substrate, vertical profiles of hydraulic conductivity and dissolved oxygen (VertiCO) are typically first sampled and then the freeze core is extracted (Negreiros et al., 2023a; Seitz, 2020).

For a VertiCO measurement, at first, a hollow standpipe is pounded approx. 0.5 m into the ground (right standpipe in Fig. 1). The standpipe has 15 vertically aligned, point-like perforations ( $\varnothing$  of 10.5 mm) at vertical equidistances of 30 mm, which are each covered with a fine metal mesh. A so-called double packer is introduced into the standpipe to create a vertically movable chamber that serves to suck up soil water at the 15 perforations without creating underpressure. Thus, the dissolved oxygen (in mg/L) and suction rates (in mL/s) can be measured at 15 points along the vertical riverbed axis. Thus, VertiCO measures the depth-explicit suction volume flow rate of a water–air mixture in the

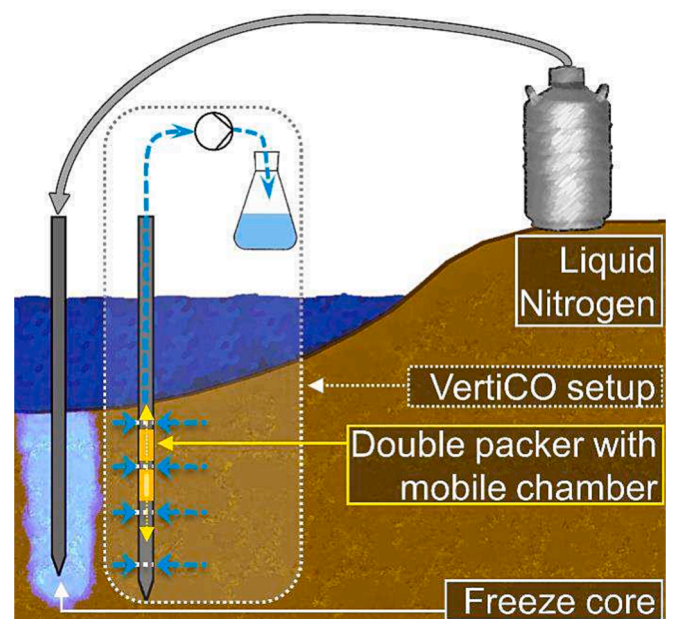


Fig. 1. The MultiPAC setup consisting of a freeze core standpipe (left) filled with liquid nitrogen, and the VertiCO standpipe (right) for suction rate and interstitial dissolved oxygen measurements (qualitative representation).

interstitial. Every measurement is repeated three times to increase the reliability of measurements.

Freeze coring is currently the only available technique for taking near-lossless mixed fine and coarse sediment samples in flowing water. To extract a freeze core, another, closed (i.e., perforation-free) standpipe with a diameter of approx. 0.05 m is driven 0.3 m to 0.4 m into the ground (left standpipe in Fig. 1) and then filled with liquid nitrogen. After 10 to 15 min, the liquid nitrogen has frozen the substrate in a radius of 0.15 m to 0.2 m and the standpipe can be pulled out of the soil, including the frozen substrate. Once melted, the extracted substrate provides an almost lossless sample serving for a precise determination of the riverbed grain size composition (Carling and Reader, 1981; Negreiros et al., 2023a; Petts et al., 1989).

### 2.1.2. Sediment characteristics

Sieving of a melted and dried freeze core provides grain size characteristics with importance to describe the state of clogging of a riverbed, notably, the  $D_{84}$  and  $D_{16}$ , and the fine sediment fraction  $FSF$ , defined as the fraction smaller than 1 mm. For characterizing the shape of the grain size distribution, the sorting coefficient  $s_0$  was defined as (Bunte and Abt, 2001):

$$s_0 = \sqrt{D_{84}/D_{16}} \quad (1)$$

In addition, the geometric standard deviation  $\sigma_{ss}$  of the grain size distribution serves to calculate the porosity  $\eta$  with the following empirical equation (Frings et al., 2011; Wooster et al., 2008):

$$\eta = 0.621 \cdot \exp(-0.457 \cdot \sigma_{ss}) \quad (2)$$

$\sigma_{ss}$  also factors into the adjusted bed-to-grain ratio  $\varphi$ , which is another parameter to characterize clogging (Huston and Fox, 2015):

$$\varphi = \frac{D_{ss}}{D_{fs}\sigma_{ss}} \quad (3)$$

$D_{fs}$  is here adapted as the geometric mean grain size of very fine sediment < 0.25 mm only, and  $D_{ss}$  is the geometric mean grain diameter of the entire sediment sample. A  $\varphi$  smaller than 27 indicates bridging (i.e., clogging), while  $\varphi > 27$  indicates unimpeded static percolation (USP), which corresponds to no clogging.

### 2.1.3. Interstitial dissolved oxygen concentration (IDOC) and hydraulic conductivity

Both interstitial dissolved oxygen concentration (IDOC) and, indirectly, hydraulic conductivity  $k_f$  are measured depth-explicitly with the VertiCO technique (Fig. 1). The IDOC has been previously used to indicate the intensity of riverbed clogging (Seitz, 2020), in particular, because an IDOC of less than 5 mg/L is lethal for many aquatic species (Gibson, 1993; Heywood and Walling, 2007). In the VertiCO setup (Fig. 1), IDOC can be determined by optode recordings of soil water samples extracted at multiple riverbed depths. While constant or falling head infiltrometers (Bouwer, 1966; Latorre et al., 2013) could directly measure  $k_f$ , the VertiCO technique requires an additional step for calculating  $k_f$ . The reasons for not using infiltrometers are to keep the impact of driving sample-destructing devices into the ground as small as possible and to derive depth-explicit  $k_f$  with VertiCO. To this end, VertiCO-based  $k_f$  requires substrate matrix information from a freeze core for a simplified, local box-like numerical model of the hyporheic zone at a measurement point. For instance, the MODFLOW software (Harbaugh, 2005) can use the measured volumetric suction rates (mL/s) as boundary conditions, it accounts for turbulent flow in the hyporheic zone to evaluate the Forchheimer equation (Ward, 1964), and it outputs depth-explicit  $k_f$ .

## 2.2. Novel fuzzy-logic method to quantify clogging

### 2.2.1. Fuzzy logic for clogging parameters

The MultiPAC parameters IDOC,  $k_f$ ,  $\eta$ , and  $FSF$  are typically used for interpreting a degree of clogging based on expert opinion (Haun et al., 2022; Negreiros et al., 2023a) in addition to the adjusted bed-to-grain ratio  $\varphi$  (Huston and Fox, 2015). Currently, classification of a clogging state in terms of words (e.g., low to strong clogging) or numbers (e.g., degrees 1 to 3) requires subjective expert assessment of multiple measured parameters or subjective mapping (Schälchli, 1992). To reduce subjectivity and agglomerate information of multiple measured parameters, this study provides a novel assessment scheme based on fuzzy logic. In contrast to Boolean logic, fuzzy logic assumes imprecise transitions between states of a natural system (Zadeh, 1965). In the framework of fuzzy logic, every observation can belong to more than one category and thus, be expressed in the form of a fuzzy vector. The fuzzy vector is a stacked representation of degrees of belongingness to classes for every observation. The degree of belongingness to classes is determined by membership functions, which are defined for every class. Such fuzzy classification enabled us to aggregate information from various sources (i.e., the literature and field data) through memberships and fuzzy rules for translating measured parameter values into degrees of clogging. Individually measured parameters can be assigned to categories, such as *low* or *high*, through membership functions. A combination of individual membership-based categories was achieved with fuzzy rules to classify multi-parametric measurements resulting from MultiPAC as *no*, *moderate*, or *strong clogging*. The following paragraphs provide details on the derivation of normative, intuitively interpretable indicators of a degree of clogging, and an amount of declogging ranging from 0 to 1.

### 2.2.2. Fuzzy membership functions

An extensive literature review determined values for five parameters ( $FSF$ ,  $k_f$ ,  $\eta$ , IDOC, and  $\varphi$ ) to inform fuzzy membership functions. Table 1 lists the parameter ranges resulting from literature review, and the detailed rationales are provided with the supplementary material. We fitted membership functions  $\mu$  (Equation (4)) of fuzzy clogging classes using the literature-based reference values (i.e., crisp thresholds) in Table 1. The membership functions *fuzzify*, that is, assign a membership  $\mu$  between 0 and 1, to each parameter for their categorization into *low* ( $\mu = 0$ ) and *high* ( $\mu = 1$ ) value ranges. For instance, an  $FSF$  of 1% corresponds to a primary *low FSF* membership. In addition,  $\varphi$  (Equation (3)) requires categories of *bridging* (surface clogging) and *USP* (no clogging).

The mathematical shape of the membership functions  $\mu$  was defined using sigmoid (i.e., S-shaped) curves, which are commonly used in fuzzy-logic applications (Rezaee et al., 2008). The Gaussian-like sigmoid curves are most suitable to emulate stochastic uncertainty in the parameter categorization (Duch, 2005). In addition, sigmoid functions feature little function derivatives at extremes along the value (*val*) axis (i.e., at 0 and 1), which means that memberships change very little in small or high-value ranges. Equation (4) shows the generic definition of a sigmoid function to describe the membership functions  $\mu_{cat,PAR}(val)$ :

$$\mu_{cat,PAR}(val) = \frac{1}{1 + e^{[c(val-b)]}} \quad (4)$$

in which  $b$  and  $c$  are shape parameters controlling the shift and stretch of the sigmoid function along the *val*-axis, respectively. The subscript *cat* refers to the categories of *low*, *high*, and *USP* and *bridging* (Table 1). The subscript *PAR* refers to the five parameters listed in Table 1. The shape parameters  $b$  and  $c$  are listed in Table 2 for the ten membership functions (two per parameter) required for the fuzzification. The two boundary values (Table 1) for each category of every parameter served to obtain  $b$  and  $c$ . The sigmoid membership functions for every parameter and category according to the parameters  $b$  and  $c$  are plotted in Fig. 2.

**Table 1**  
Literature-based values used for the categories to fit the membership functions  $\mu$  (Equation (4)).

Parameter	Category	Value	$\mu$ (-)	(Sources)
Fine sediment fraction $FSF$ (%)	high	20	0.90	(Reiser and White, 1988)
		8	0.10	(Heywood and Walling, 2007)
	low	1	0.99	New definition
		11	0.10	(Negreiros et al., 2023a)
Bed-to-grain ratio $\varphi$ (-)	Unimpeded static percolation (USP) bridging	44.8	0.90	(Huston and Fox, 2015)
		27	0.10	(Mayar et al., 2022)
		10	0.99	(Huston and Fox, 2015)
		27	0.10	(Huston and Fox, 2015)
Porosity $\eta$ (%)	low	6	0.90	(Maridet and Philippe, 1995)
		15	0.10	(Descloux et al., 2010)
	high	26.2	0.90	(Negreiros et al., 2023a)
		15	0.10	(Descloux et al., 2010)
Hydraulic conductivity $k_f$ (m/s)	low	2.00E-5	0.90	(Datry et al., 2015)
		5.56E-3	0.10	(Gibson, 1993; Rubin, 1998; Wickett, 1954)
	high	2.78E-2	0.99	(Chapman, 1988)
		1.00E-4	0.10	(Blaschke et al., 2003)
Interstitial dissolved oxygen concentration IDOC (mg/L)	low	1	0.90	New definition
		6	0.10	(Gibson, 1993; Heywood and Walling, 2007; Sowden and Power, 1985)
	high	10	0.90	(Lindroth, 1942)
		3	0.10	(Rubin and Glimsäter, 1996)

**Table 2**  
Shape parameters  $b$  and  $c$  of the sigmoid membership functions (Equation (4)) for the fuzzification of the input parameters.

Parameter (PAR)	Category (CAT)	$b$	$c$
$FSF$ (clogging)	high	14.00	0.37
$FSF$ (no clogging)	low	7.97	-0.66
$\varphi$ (no clogging)	USP	35.90	0.25
$\varphi$ (clogging)	bridging	21.50	-0.40
$\eta$ (clogging)	low	10.50	-0.49
$\eta$ (no clogging)	high	20.60	0.39
$k_f$ (clogging)	low	0.0038	-1226.1
$k_f$ (no clogging)	high	0.0010	2534.5
IDOC (clogging)	low	3.50	-0.88
IDOC (no clogging)	high	6.50	0.63

2.2.3. Aggregation of memberships

To aggregate (i.e., combine) the parameter-specific membership values into fuzzy classes of *strong clogging* (SC), *moderate clogging* (MC), and *no clogging* (NC), we defined fuzzy rules (cf. Table 3 below). Thus, every MultiPAC location is assigned a membership  $\mu_{SC}$ ,  $\mu_{MC}$ , and  $\mu_{NC}$  as a function of the logical operations  $\mu_{SC,i}$ ,  $\mu_{MC,i}$  and  $\mu_{NC,i}$  in the last column of Table 3. The logical rules with subscripts  $i$  apply a fuzzy AND operator, which logically represents a minimum to derive  $\mu_{SC,i}$ ,  $\mu_{MC,i}$  and  $\mu_{NC,i}$  as a function of  $\min(\mu_{category,PAR}, \mu_{category,PAR})$ . Next, fuzzy OR operators logically choose the maximum of  $\mu_{SC,i}$ ,  $\mu_{MC,i}$  and  $\mu_{NC,i}$  to derive the final class memberships to  $\mu_{NC}$  (no clogging),  $\mu_{MC}$  (moderate clogging),

and  $\mu_{SC}$  (strong clogging). Note that the rules listed in Table 3 are based on literature-available data (Table 1) to inform fuzzy sets. Based on the literature and to the author’s best knowledge, there were no rules available for some combinations, such as IDOC is low and  $k_f$  is low (inverse of rule NC,1).

2.2.4. Defuzzification: Depth-explicit degree of clogging

Defuzzification is the translation of a fuzzy membership back into a numeric value of a (normalized) degree of clogging based on the defuzzification membership functions plotted in Fig. 3. The defuzzification (denoted by subscript  $dfz$ ) curves  $\mu_{NC,dfz}$  (no clogging) and  $\mu_{SC,dfz}$  (strong clogging) are also sigmoid functions according to Equation (4) with the shape parameters in Table 4. Note that the moderate-clogging defuzzification function for  $\mu_{MC,dfz}$  (moderate clogging) corresponds to a (Gaussian) bell curve with a mean at  $\zeta = 0.5$  and a standard deviation of 0.083.

The defuzzification starts with calculating the areas below the calculated class memberships  $\mu_{SC}$ ,  $\mu_{MC}$ , and  $\mu_{NC}$ . For every defuzzification curve  $\mu_{NC,dfz}$ ,  $\mu_{MC,dfz}$ , and  $\mu_{SC,dfz}$  horizontal lines (constant values) can be plotted on the  $y$ -axis ( $\mu$ ) values of calculated  $\mu_{NC}$ ,  $\mu_{MC}$ , and  $\mu_{SC}$ . The intersection of these horizontal lines with the corresponding defuzzification curves ( $\mu_{NC,dfz}$ ,  $\mu_{MC,dfz}$ , and  $\mu_{SC,dfz}$ , respectively) and the  $x$ -axis ( $\mu = 0$ ) delineate three areas that are unified into one area. Next, we computed the centroid of the union of all areas (i.e., the coordinates of the centroid-of-area). The  $x$ -coordinate of the unified area represents a degree of clogging that requires scaling for interpretability (de Oliveira, 1995; Patro and Sahu, 2015). Only with scaling, a measurement data set with 100-percent membership in  $\mu_{NC}$  (no clogging) and 0-percent membership in  $\mu_{MC}$ , and  $\mu_{SC}$  has the intuitively expected degree of clogging of zero. Without scaling, the centroid-of-area of the no-clogging defuzzification curve  $\mu_{NC,dfz}$  is approx. at  $x = 0.2$ , which means that the minimum possible degree of clogging was 0.2. Vice versa, at the upper end of the clogging spectrum, *fully clogged* should correspond to a degree of clogging of 1.0. To enable such an intuitive interpretation of the degree of clogging, we scaled the calculated  $x$ -coordinate of the centroids-of-area. That is, we scaled the  $x$ -coordinate of the unified area-of-centroid by the  $x$ -distance between the centroids-of-area of the defuzzification curves  $\mu_{NC,dfz}$  and  $\mu_{SC,dfz}$ , which represent the minimum and maximum  $x$ -values in this system of coordinates, respectively. Thus, we yielded a normalized degree of clogging  $\zeta$  ranging from 0 (*no clogging*) to 1 (*fully clogged*). Calculous implementations in Python code are provided with the code documentation prepared along with this study (Negreiros et al., 2023b; Schwindt et al., 2023). The sensitivity of  $\zeta$  regarding the literature-based values for deriving the membership curves (Table 1) was additionally examined and is provided with the results.

Fig. 3 exemplifies the defuzzification to yield the normalized degree of clogging at a fictive measurement point, where  $FSF = 13.65\%$ ,  $k_f = 2.4E-03$  m/s,  $\eta = 0.2$ , IDOC = 12.2 mg/L, and  $\varphi = 30.6$ . The measured values lead to fuzzy memberships of  $\mu_{NC} = 0.97$ ,  $\mu_{MC} = 0.85$ , and  $\mu_{SC} = 0.47$ . The calculation of areas between the horizontal lines of the fuzzy memberships and the defuzzification curves ( $\mu_{NC,dfz}$ ,  $\mu_{MC,dfz}$  and  $\mu_{SC,dfz}$ ) define a unified area with a centroid  $x$ -coordinate of 0.47. Scaling by the  $x$ -distance between the centroids-of-area of  $\mu_{NC,dfz}$  ( $x = 0.2$ ) and  $\mu_{SC,dfz}$  ( $x = 0.85$ ) curves results in a normalized degree of clogging  $\zeta = (0.47 - 0.2)/(0.85 - 0.2) = 0.42$ .

2.2.5. Depth-integrated amount of declogging

In a morphodynamically active river, the riverbed level can be expected to change over time. Therefore, when comparing depth-explicit profiles of IDOC and  $k_f$  from different measurement times using fuzzy rules, it is necessary to install MultiPAC at different bed levels at different observation times and combine them with bulk freeze core parameters. To address both bed level change and bulkiness of freeze core parameters, this study introduces a new metric, the normalized Area Between Profiles ( $nABP$ ). For each parameter (here, IDOC or  $k_f$ ),

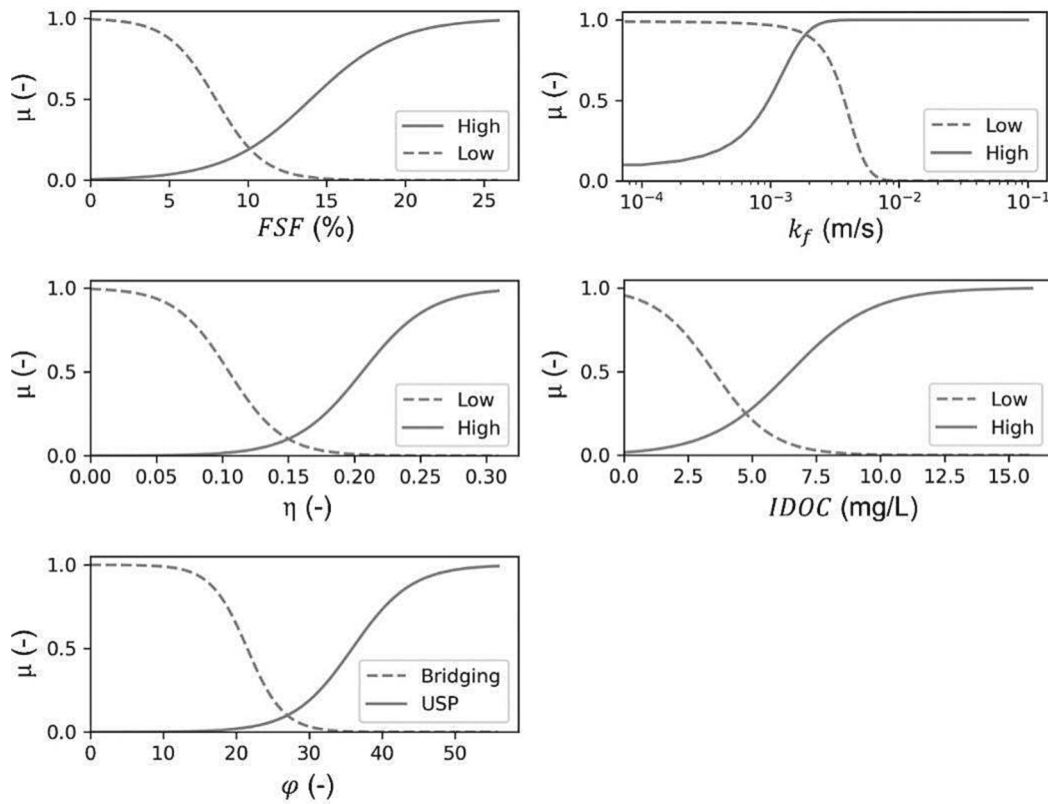


Fig. 2. Membership functions  $\mu$  for the fuzzification of each parameter into fuzzy sets.

the  $nABP$  is calculated as the difference between the area under earlier ( $t_0$ ) and later ( $t_1$ ) recorded profiles of the parameter (i.e., comparison of curves  $PAR_{t_0}(z)$  and  $PAR_{t_1}(z)$ ), normalized by the difference in vertical position relative to the riverbed depth axis ( $z$ ). This normalization factor is determined by the difference in depth between the deepest measuring level ( $z_2$ ) and the level closest to the surface at each MultiPAC point ( $z_1$ ), and is given by  $(z_2 - z_1)^{-1}$ . Thus, the depth normalization accounts for the varying depths of the VertiCO standpipes relative to the surface elevation of the riverbed. The  $nABP$  for a parameter  $PAR$  integrates the area starting from  $z_1$  down to  $z_2$  at the same MultiPAC measurement point from two observation times ( $t_0$  and  $t_1$ ) with respect to  $z$ :

$$nABP(PAR) = \int_{z_1}^{z_2} (PAR_{t_1}(z) - PAR_{t_0}(z)) dz \bullet (z_2 - z_1)^{-1} \quad (5)$$

As a result, positive  $nABP$  indicates an increase and negative  $nABP$  indicates a decrease in IDOC or  $k_f$  because of any event between  $t_0$  and  $t_1$ . The MultiPAC points from observation times  $t_0$  and  $t_1$  should spatially be at the same point (e.g., measured with a differential global positioning system, DGPS) within a 0.5-m radius, but not at exactly the same positions because the freeze core from  $t_0$  could affect the sample at  $t_1$ .

Finally, to test whether clogging has been reduced by a restoration action between  $t_0$  and  $t_1$ , we introduce the normative, intuitively interpretable amount of declogging  $\Delta\zeta$ :

$$\Delta\zeta = -nABP(\zeta) = - \int_{z_1}^{z_2} (\zeta_{t_1}(z) - \zeta_{t_0}(z)) dz \bullet (z_2 - z_1)^{-1} \quad (6)$$

where  $\zeta_{t_0}$  and  $\zeta_{t_1}$  result from the fuzzy inference system applied to MultiPAC measurements from the two observation times  $t_0$  and  $t_1$ . Thus,  $\Delta\zeta$  is defined as the difference in  $\zeta$  from  $t_0$  minus  $t_1$ . That is, a positive  $\Delta\zeta$  indicates declogging.

### 2.3. Declogging experiment with large wood

#### 2.3.1. Experimental design

To test the efficacy of the new fuzzy-logic method for identifying potential declogging effects of large wood (LW) placements, we conducted a hands-on morphologically effective flushing experiment at an artificial, morphodynamically active gravel-bed fish pass. The fish pass was installed between 2018 and 2020 to bypass a hydropower plant on the Inn River (Germany, lat. 48.29160, long. 13.15852, map in the [supplementary material](#)) and features forced meanders, pool-riffle sequences, gravel bars, and swales, creating valuable habitats for indigenous gravel-spawning fish like the Danubian gudgeon (*Romanogobio uranoscopus*) or Danube salmon (*Hucho hucho*) (Zauner et al., 2020). The inlet and outlet of the 2.6-km-long fish pass had an elevation difference of 10 m, and the local bottom slope at the LW placements was 4.7‰. The channel width varied between approximately 5 m (pools) and 10 m (riffles) at baseflow ( $2 \text{ m}^3/\text{s}$ ). Coarse sediment deposits, sourced by a downstream sediment trap, were installed in the fish pass before the flushing event. These deposits were designed to be mobilized by the artificial flushing event to promote self-maintenance of the morphological units (Sawyer et al., 2010; Woodworth and Pasternack, 2022), renewing the valuable habitats for gravel-spawning fish (Harrison et al., 2011, 2019).

The artificial flood to trigger morphological self-maintenance corresponded to bankfull discharge, with peak discharge sufficient for mobilizing surface grain sizes up to 0.3 m in the fish pass (according to information from the operators). Thus, the flushing event was designed to break up potentially armored and clogged riverbed patches, and initiate fine sediment removal. Since the construction of the fish pass, such flushing had already been conducted once with a duration of 7 h. This study adapted the design of the previous flushing event in which the discharge was increased at the fish pass inlet from the baseflow of  $2 \text{ m}^3/\text{s}$  to a peak flow of  $9.7 \text{ m}^3/\text{s}$  over approx. 45 min and similarly reversed at the end of the flushing event (hydrograph included in the [supplementary](#)

**Table 3**  
Fuzzy inference system including its fuzzy aggregation rules for determining the membership of the clogging classes.

Class	Rule number	Fuzzy rule	Rationale	Logical operation
Strong Clogging (SC)	SC,1	If $k_f$ is low AND $FSF$ is high	$k_f$ decreases rapidly when $FSF$ increases and drops to 0 when $FSF$ exceeds 20% (Descloux et al., 2010).	$\mu_{SC,1} = \min(\mu_{low,kf}, \mu_{high,FSF})$
	SC,2	If $FSF$ is high AND porosity is low	High $FSF$ means that $\eta$ is low; vice versa $\eta$ may be high or low when $FSF$ is low (Maridet et al., 1992).	$\mu_{SC,2} = \min(\mu_{high,FSF}, \mu_{low,\eta})$
	SC,3	If $\varphi$ indicates bridging AND $k_f$ is low	Clogging is likely if $\varphi$ indicates bridging (Huston and Fox, 2015) regardless of other parameters.	$\mu_{SC,3} = \min(\mu_{bridging}, \mu_{low,kf})$
	SC	<b>If SC-1 OR SC-2 OR SC-3 is TRUE</b>		$\mu_{SC} = \max(\mu_{SC,1}, \mu_{SC,2}, \mu_{SC,3})$
Moderate Clogging (MC)	MC,1	If $k_f$ is low AND IDOC is high	When IDOC is high and $k_f$ is low, the riverbed is not considered to be strongly clogged, otherwise oxygen-rich surface water could not infiltrate into the hyporheic zone.	$\mu_{MC,1} = \min(\mu_{low,kf}, \mu_{high,FSF})$
	MC,2	If $FSF$ is high AND $k_f$ is NOT low	Hyporheic pores can be clogged by sand with high $\eta$ and $k_f$ .	$\mu_{MC,2} = \min(\mu_{high,FSF}, 1 - \mu_{low,kf})$
	MC	<b>If MC-1 OR MC-2 is TRUE</b>		$\mu_{MC} = \max(\mu_{MC,1}, \mu_{MC,2})$
No Clogging (NC)	NC,1	If IDOC is high AND $k_f$ is high	High IDOC is unlikely to occur in clogged riverbeds. Thus, if $k_f$ is also high, good exchange conditions are assumed (i.e., no clogging).	$\mu_{NC,1} = \min(\mu_{high,IDOC}, \mu_{high,kf})$
	NC,2	If $k_f$ is high AND $FSF$ is low	If both $k_f$ and $FSF$ indicate clogging, but IDOC (or other parameters) is low, downwelling is likely to occur in the hyporheic zone.	$\mu_{NC,2} = \min(\mu_{high,kf}, \mu_{low,FSF})$
	NC,3	If $\varphi$ indicates USP AND $k_f$ is high	Opposite of SC,3.	$\mu_{NC,3} = \min(\mu_{USP}, \mu_{high,kf})$
	NC	<b>If NC-1 OR NC-2 OR NC-3 is TRUE</b>		$\mu_{NC} = \max(\mu_{NC,1}, \mu_{NC,2}, \mu_{NC,3})$

material). The peak discharge was constant for 8 h and verified with an acoustic Doppler current profiler (Sontek M9) that also provided velocity measurements, which were used to estimate the maximum Froude number being in the subcritical range (maximum of approx. 0.6). The flushing event in this study was run after LW installation, and we made pre- ( $t_0$ ) and post- ( $t_1$ ) flushing event MultiPAC measurements. On January 25, 2022, LW was placed in the fish pass and a pre-flushing measurement campaign was conducted between January 31 and February 2, 2022. The flushing event occurred on February 3, 2022. A post-flushing measurement campaign was performed between February

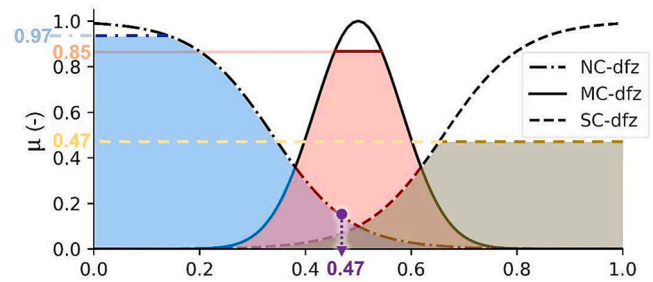


**Fig. 3.** The three defuzzification membership functions with an exemplary defuzzification of class memberships through the centroid-of-area with fictional values of  $\mu_{NC-dfz} = 0.97$  (blue),  $\mu_{MC-dfz} = 0.85$  (red) and  $\mu_{SC-dfz} = 0.47$  (yellow) yielding a unified centroid-of-area at an x-coordinate of 0.47 (purple). Scaling by the centroid-of-area coordinates of the blue, red, and yellow areas leads to a normalized degree of clogging of  $\zeta = 0.42$ . (For interpretation of the references to colour in this figure legend, the reader is referred to the web version of this article.)

**Table 4**  
Shape parameters b and c in for the sigmoid defuzzification functions (Equation (4)).

Class (Parameter PAR)	b	c
No clogging ( $\mu_{NC-dfz}$ )	0.34	-13.58
Strong clogging ( $\mu_{SC-dfz}$ )	0.66	13.58

7 and 11, 2022.

### 2.3.2. Placement and design of wood logs

The LW logs had a length of 4.8 m and an average diameter of 0.7 m (see supplementary material). Each log was fixed with four vertical chocks and steel cables, making this technically an engineering logjam (ELJ). The upstream log was referred to as log A and the downstream as log B. Log A was emergent and log B was submerged at a baseflow of 2 m<sup>3</sup>/s. However, both logs were emergent at the minimum flow of 0.5 m<sup>3</sup>/s for the installation (Fig. 2) and MultiPAC measurements, but submerged during the flushing event.

### 2.3.3. Measurement devices

MultiPAC measurements were taken upstream and downstream of both logs (positions in Fig. 4) before ( $t_0$ ) and after ( $t_1$ ) the flushing event. In addition,  $t_0$  and  $t_1$  MultiPAC measurements were made at a reference point located about 140 m upstream of log A, with comparable flow characteristics but without the influence of LW. The position of the reference MultiPAC point is mapped in the supplementary material. The IDOC was recorded using a HACH HQ30d optode. All measurement locations were recorded using a Leica DGPS (type RX1250TC). The measurement parameters resulting from MultiPAC are summarized in Table 5, including measurement precisions. Additionally, aerial imagery was captured using a dji Phantom 4RTK drone.

To provide evidence for the accuracy of the hypothesis that LW locally relieves clogging, the amount of declogging  $\Delta\zeta$  (Equation (6)) should be greater at the four MultiPAC measurements in the vicinity of the logs than at a reference point. Before using the new fuzzy-logic method to calculate  $\Delta\zeta$ , the results show the evolution of the five measured quantities  $FSF$ ,  $\eta$ ,  $\varphi$ , IDOC, and  $k_f$  in the context of clogging characteristics.  $\Delta\zeta$  was also considered in light of changes in the grain size distributions and topographic change  $\Delta z$ , which was measured with the Leica DGPS at the centers of the MultiPAC points (Fig. 4).

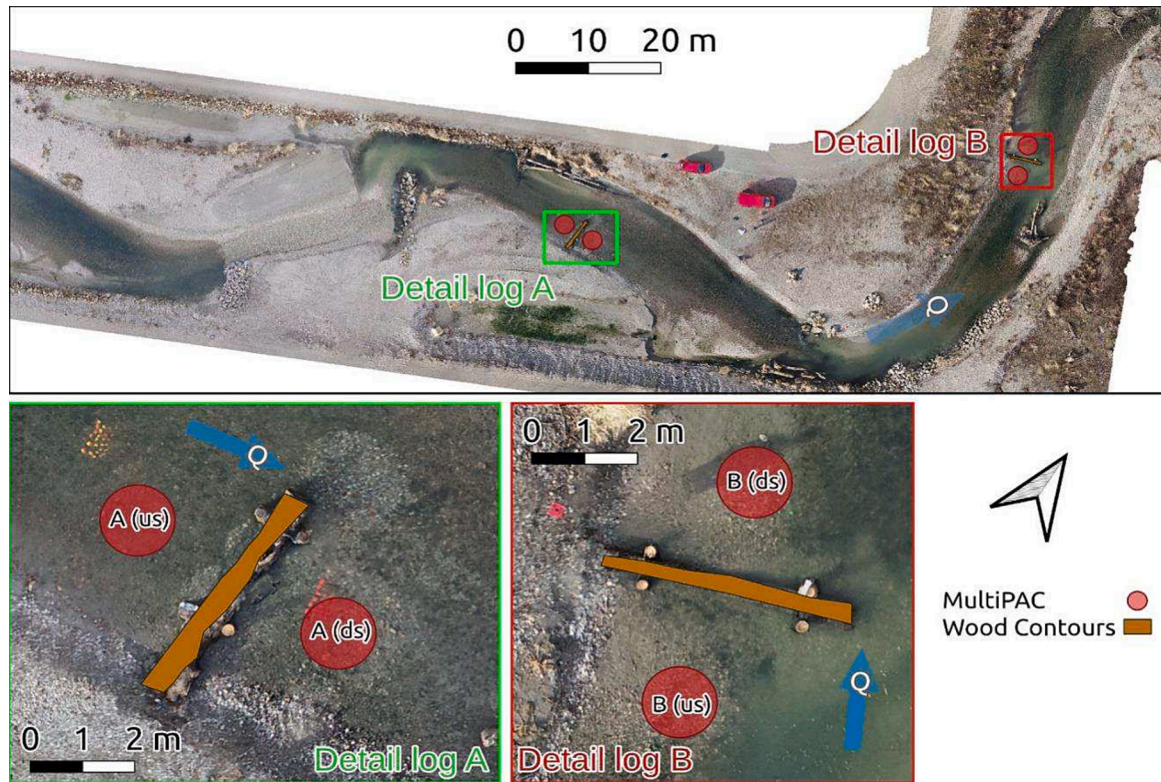


Fig. 4. Top view of the field site with background drone imagery taken after the flushing event, showing the position of the two logs and MultiPAC points (i.e., freeze cores and VertiCO), which are labeled according to the closest log (A and B) and relative position upstream (us) and downstream (ds) to the log.

**Table 5**  
Measurement quantities, target parameters, precision, and devices/techniques used in this study (Fig. 4).

Measurement Quantity	Target Parameters	Precision	Device/Technique
Interstitial dissolved oxygen concentration	IDOC	±0.15 mg/L	VertiCO (MultiPAC)
Hydraulic conductivity	$k_f$	±5.5E-04 m/s	VertiCO (MultiPAC)
Substrate sediment grain sizes	$\varphi, \eta, FSF, s_0$	< 1% <sup>‡</sup>	Freeze core (MultiPAC)
Topographic change	$\Delta z$	±0.02 m	DGPS

<sup>‡</sup> based on (Seitz, 2020).

### 3. Results

#### 3.1. MultiPAC measurements

##### 3.1.1. Grain size characteristics

The grain size characteristics  $D_{10}$  (representative for fine sediment),  $D_{50}$  (representative for bulk substrate), and sorting coefficient  $s_0$

(incorporating  $D_{16}$  and  $D_{84}$ ) measured before and after the flushing event are listed in Table 6. At log A,  $D_{10}$  and  $D_{50}$  increased with the flushing event, while  $s_0$  decreased. Thus, the grain size distribution at log A became coarser and narrower with the flushing. At log B,  $D_{10}$  experienced a little decrease downstream, and no detectable change upstream.  $D_{50}$  slightly decreased upstream of log B with little to no change downstream. Upstream of log B,  $s_0$  decreased a little, but downstream,  $s_0$  increased. At the reference point,  $D_{10}$  did not change while  $D_{50}$  and particularly  $s_0$  increased, which corresponds to a little coarser and wider grain size distribution after the flushing.

##### 3.1.2. Fine sediment fraction (FSF) and porosity

The freeze core samples at log A had higher FSF (22.0% to 34.5%) and lower  $\eta$  (0.14 to 0.16) compared with log B, where the FSF was between 18.1% and 13.7%, and  $\eta$  between 0.19 and 0.21 (Fig. 5). The observations at log A are related to the deposition of coarse sediment during the flushing event (Table 6). The arrows indicating changes during the flushing event in Fig. 5 suggest a decrease in the FSF and an increase in  $\eta$  at log A, which corresponds to declogging in line with the coarsening of grain sizes. The inverse relationship evolution between the FSF and  $\eta$  as observed at log A was expected, but not evident at log B, where an increase in  $\eta$  with little change in the FSF was related to the accumulation of sand fractions ( $D_{10}$  in Table 6). The small changes in the

**Table 6**  
Measured grain size characteristics  $D_{10}$ (in mm),  $D_{50}$ (in mm), sorting coefficient  $s_0$  (-), FSF (%), and  $\eta$  (-) based on freeze cores at LW placements (Fig. 4) and the reference point.

Location	$D_{10}$	$D_{50}$	$s_0$	Before ( $t_0$ )		$D_{10}$	$D_{50}$	$s_0$	After ( $t_1$ )	
				FSF	$\eta$				FSF	$\eta$
A(us)	0.1	10.4	13.2	29.8	0.14	0.2	13.3	11.0	22.0	0.16
A(ds)	0.1	8.0	12.4	34.5	0.14	0.1	9.3	11.5	30.2	0.15
B(us)	0.4	16.9	4.8	13.7	0.21	0.4	14.3	4.5	13.8	0.21
B(ds)	0.4	14.9	6.4	16.6	0.20	0.3	15.2	9.2	18.1	0.19
Reference	0.4	9.7	6.2	17.7	0.21	0.4	10.3	8.1	19.5	0.20

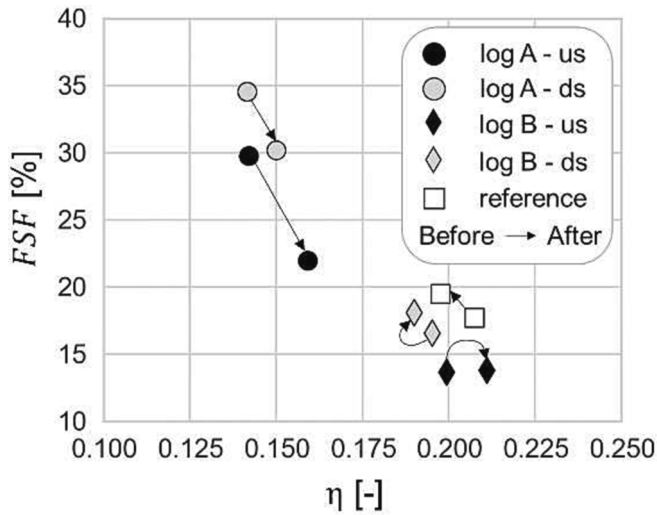


Fig. 5. Measured fine sediment fractions ( $FSF$ ) < 1 mm plotted against porosity  $\eta$ , based on freeze core samples. The arrows indicate parameter evolution during the flushing event.

$FSF$  and  $\eta$  were close to the device precision (Table 5) upstream of log B. Downstream of log B, the increase in the  $FSF$  was high, but the decrease in  $\eta$  was below the level of precision. At the reference point, the porosity decreased a little from 0.21 to 0.20, and the  $FSF$  increased from 17.7% to 19.5%.

### 3.1.3. Bed-to-grain ratio

The bed-to-grain ratio  $\phi$ , calculated from freeze core measurements using Equation (3), mostly fell into the bridging range (Fig. 6). The only exception was upstream of log B, where  $\phi$  was considerably larger than at other points, with values around 30, primarily attributable to the USP range. The slight improvements in  $\phi$  at log A, before and after the flushing event, still fell into the bridging region indicating more clogging. At the reference point, the already low  $\phi$  decreased sharply during the flushing event, moving toward the bridging region (i.e., more clogging).

### 3.1.4. Interstitial dissolved oxygen content (IDOC) and hydraulic conductivity

Log A was surrounded by greater heterogeneity in vertical profiles of IDOC and  $k_f$  before and after the flushing event compared to log B (Fig. 7, with *us* and *ds* locations indicated in Fig. 4). At log B, pre-flushing IDOC and  $k_f$  were generally higher compared to the low IDOC (<8 mg/L) and  $k_f$  (<3E-4 m/s) at log A suggesting stronger sub-surface clogging at log A. Still, most  $k_f$  measurements were relevant downstream of log A and close to the surface upstream of log A,

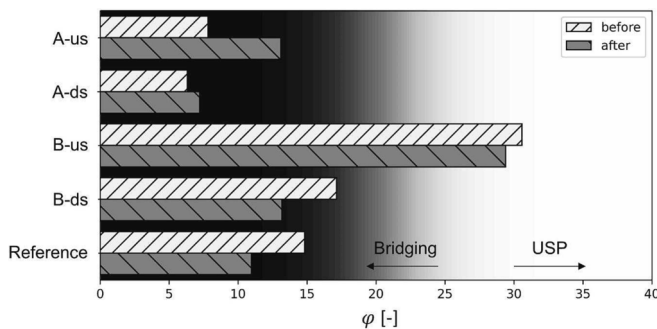


Fig. 6. The bed-to-grain ratio  $\phi$  (Equation (3)) upstream (*us*) and downstream (*ds*) of logs A and B, and at the reference point with indication of bridging and unimpeded static percolation (USP) ranges.

compared with the device precision of 5.5E-5 m/s (cf. Table 5).

At the reference point, post-flushing  $k_f$  were in the order of 1.0E-2 at a riverbed depth of 0.15 m and dropped to less than 1.0E-3 in deeper layers. Pre-flushing  $k_f$  were not available for the reference point because of a device failure. Before the flushing event, the IDOC was 12.1 mg/L close to the surface and had a minimum of 11.3 mg/L at the deepest measurement of the VertiCO standpipe (0.27 m). After the flushing event, the highest IDOC at the bed surface had slightly increased to 12.6 mg/L but a minimum of 10.6 mg/L was measured at a riverbed depth of 0.21 m.

## 3.2. Fuzzy clogging indicators

### 3.2.1. Depth-explicit degree of clogging

The vertical profiles of the normalized degree of clogging  $\zeta$  suggest a decrease in the degree of clogging upstream of log A (A-*us*, Fig. 8a), which was related to the deposition of coarse sediment described above. Downstream of log A (A-*ds*, Fig. 8a), the degree of clogging experienced fewer changes. The  $\zeta$  values at log A were in the range of 0.6 to 0.96 after the flushing event, with the smallest  $\zeta$  close to the riverbed surface. The  $\zeta$  values in the deeper riverbed upstream of log A fell into the *strong clogging* class (as per the defuzzification function in Fig. 3), where the degree of clogging decreased after the flushing event. Additionally, downstream of log A, declogging occurred close to the riverbed surface (inclination towards  $\zeta = 0.6$ ), which can be related to the log-driven morphodynamic change patterns. At log B (Fig. 8b), the degree of clogging showed little variation over depth, and it was more pronounced downstream of the log. The minimum and maximum of  $\zeta$  at log B were 0.4 and 0.65, respectively, indicating *moderate clogging* according to the fuzzy inference system. At the reference point (Fig. 8c), the vertical profiles of the degree of clogging suggest slightly more pronounced clogging after the flushing event, mainly driven by the IDOC in riverbed depths between 0.12 m and 0.27 m. The supplementary material provides a table containing all input data and the calculated degrees of clogging  $\zeta$  along with fuzzy memberships to the clogging classes of *no clogging* (NC), *moderate clogging* (MC), and *strong clogging* (SC).

Uncertainties in the literature-based input values used for interpolating the membership functions (“value” column in Table 1) propagate through the shape parameters of the sigmoid curves (Table 2 and Table 4) and thus, the judgement of the fuzzy rule system (Table 3). To assess the uncertainty involved in the fuzzy inference system, Fig. 8 shows the maximum variances in  $\zeta$  (gray-shaded areas) in response to  $\pm 10\%$  variations in the input values (“value” column in Table 1). The detailed  $\zeta$  variations as a function of individual input value variations are provided in comprehensive tables in the supplementary material. The maximum absolute  $\zeta$  deviation of 0.04 (9.8%) occurred at log B (upstream, after the flushing), at a riverbed depth of 0.15 m, where the absolute  $\zeta$  value was 0.41. The maximum percentage deviation of  $\zeta$  was 10.4% (absolute value  $0.40 \pm 0.042$ ), also upstream of log B, but before the flushing event and at a riverbed depth of 0.12 m. In both cases, the uncertainty was driven by the input ( $\mu$ ) values for defining the membership to “high  $FSF$ ”. On average, the  $\zeta$  deviation was 3.4%, which was smaller than the considered 10% uncertainty in the input values. Therefore, the fuzzy inference system tends to rather dampen potential errors in the assumptions for deriving the fuzzy indicators, and reduces the vulnerability of  $\zeta$  regarding uncertainty of the input ( $\mu$ ) values for interpolating the membership functions.

### 3.2.2. Depth-integrated amount of declogging

The trends in the amount of declogging  $\Delta\zeta$  suggest an ecological improvement (i.e., less clogging) in the vicinity of the logs and degradation (i.e., more clogging) at the reference point (first column in Table 7). Positive  $\Delta\zeta$  indicates that the flushing event caused declogging, assessed as a function of  $nABP(IDOC)$ ,  $nABP(k_f)$ ,  $\Delta\eta$ ,  $\Delta\phi$ , and  $\Delta FSF$  (Equation (6)). In addition to these five parameters, we accounted for

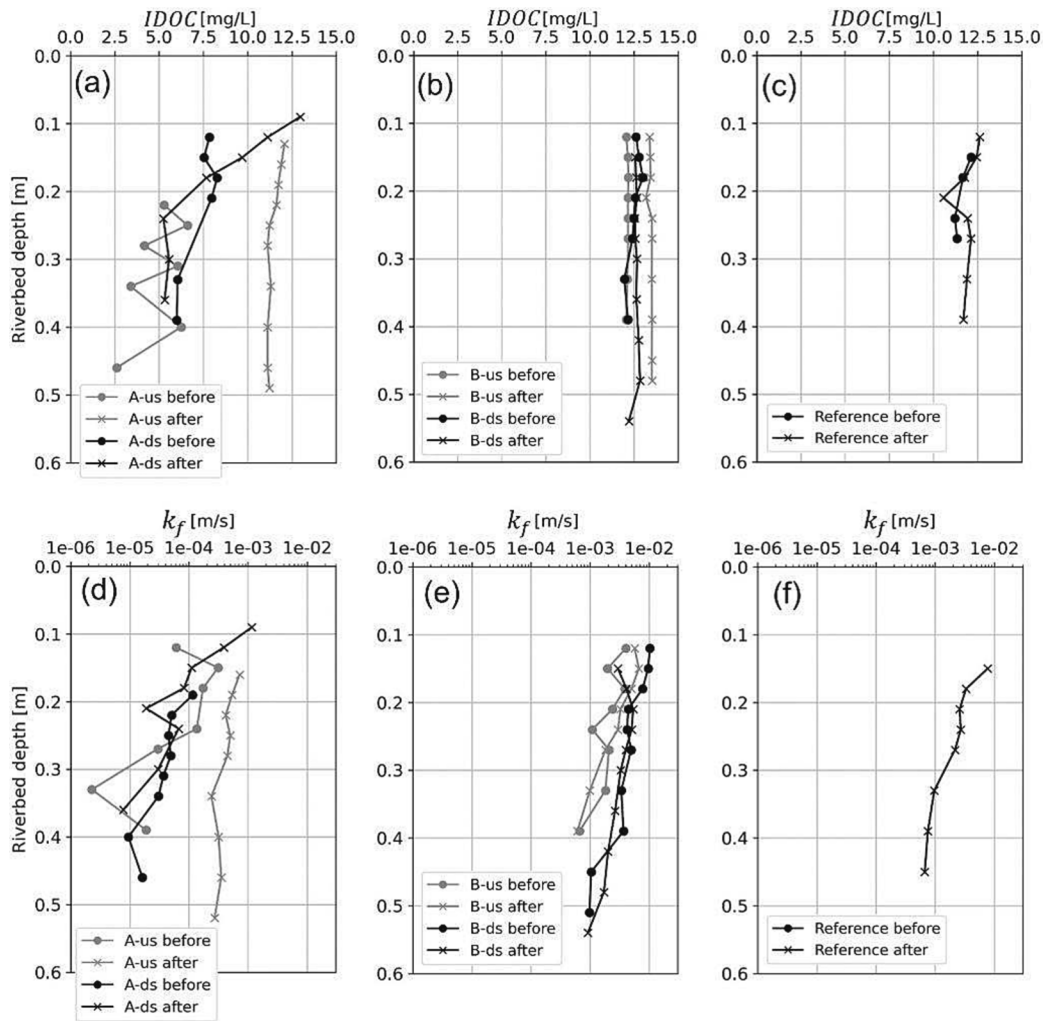


**Fig. 7.** Vertical profiles of interstitial dissolved oxygen concentration, IDOC (a-c), and hydraulic conductivity,  $k_f$  (d-f), measured in the riverbed, upstream (us), and downstream (ds) of the emergent log A (a, d) and submerged log B (b, e), and at the reference point (c, d). The profiles served for calculating  $nABP(IDOC)$  and  $nABP(k_f)$  according to Equation (5).

DGPS-measured topographic change  $\Delta z$ , which was found to be  $0.2 \pm 0.02$  m upstream of log A, and  $0.1 \pm 0.02$  m upstream of log B. Downstream of logs A and B,  $\Delta z$  was  $0.02 \pm 0.02$  m (i.e., insignificant) and  $0.03 \pm 0.02$  m, respectively. Also, deep scour pools developed at the tips of the logs, which can be seen on a scour pool map provided in the [supplementary material](#). At the reference point,  $\Delta z$  was  $-0.07 \pm 0.02$  m, indicating erosion and the only location where clogging became slightly more pronounced (i.e., negative  $\Delta \zeta$ ) after the flushing event.

The  $nABP(IDOC)$  and  $nABP(k_f)$  were calculated by comparing the IDOC and  $k_f$  profile evolution caused by the flushing event, as shown in [Fig. 7](#). Both  $nABP(IDOC)$  and  $nABP(k_f)$  were higher upstream of the logs and, in particular, after the flushing event. In contrast, the downstream measurements at both logs showed little to no change or even a decrease in  $nABP(IDOC)$  and  $nABP(k_f)$ . Positive  $nABP(IDOC)$  and  $nABP(k_f)$  upstream of the logs point to declogging. Conversely, negative  $nABP(IDOC)$  and  $nABP(k_f)$  values suggest that the logs caused slight clogging in their wake (i.e., downstream). However, the areas between pre and post-flushing  $k_f$  profiles were above the device precision only at log B with  $nABP(k_f) > 5.5E-5$  m/s, and could not be evaluated at the reference point because of the device failure in the pre-flushing survey. The net increase in  $nABP(IDOC)$  and  $nABP(k_f)$  upstream of the logs resulted from the flushing event, which also led to narrower distributed grain size distributions, and upstream of log A also to coarse bedload deposition ([Table 6](#)). In contrast, downstream of the logs, measurements

showed a net decrease in  $k_f$  ( $nABP(k_f) < 0$ ).

The changes in  $FSF$  and  $\eta$  correspond to prominent declogging at log A and almost undetectable changes at log B, where most measurements were close to the measurement device precision ([Table 5](#)). In addition, while most measurements summarized in [Table 7](#) were above the precision thresholds, the changes in porosity  $\Delta \eta$  downstream of both logs and at the reference point were not significant. However, the changes in the bed-to-grain ratio  $\Delta \phi$  were high, except for the measurement point downstream of log A. The bed-to-grain ratio  $\phi$  predominantly indicated bridging, which represents clogged conditions, particularly downstream of log A, and indicates that fine sediment clogged (bridged) the sediment matrix. The only exception was upstream of log B, where  $\phi$  primarily fell into the USP range ([Fig. 6](#)). Thus, the improvements in  $\phi$  at log A occurred in a low- $\phi$  region, while the high- $\phi$  region upstream of log B deteriorated slightly after the flushing event. The reference point exhibited a negative  $\Delta \phi$ , which was decisive for that it was the only point classified as more clogged after the flushing event ( $\Delta \zeta < 0$ ).

## 4. Discussion

### 4.1. Relevance of the fuzzy inference system and indicators

A fuzzy inference method is advantageous for assessing clogging

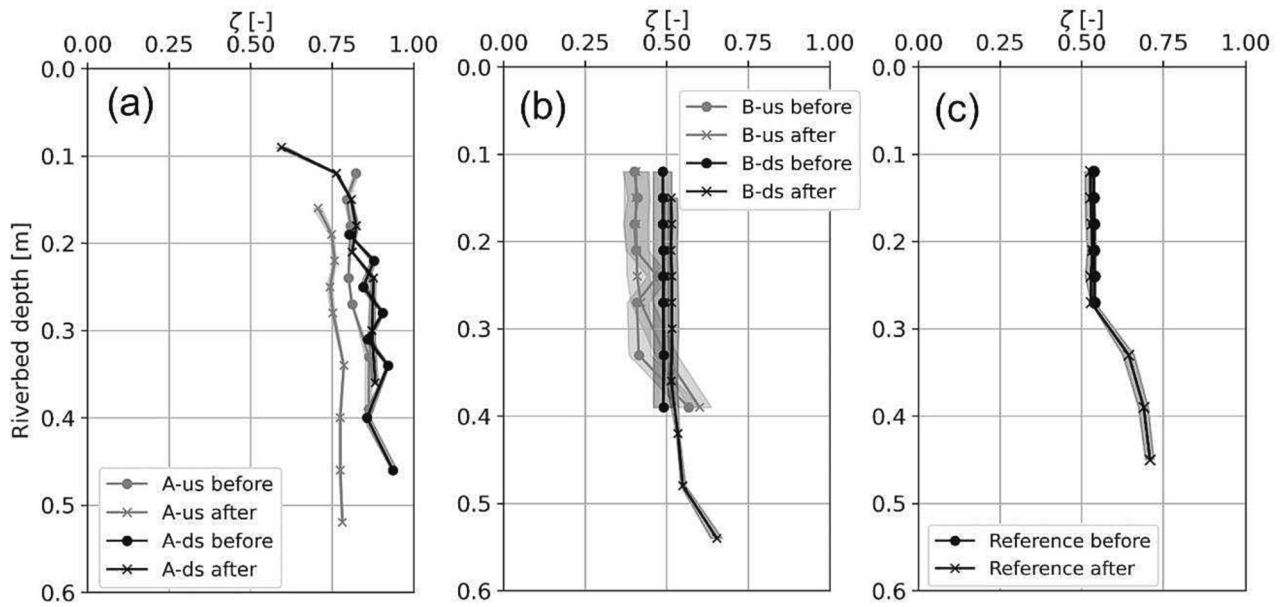


Fig. 8. Calculated profiles of the normalized degree of clogging  $\zeta$  along the riverbed depth using the fuzzy inference system for upstream (us) and downstream (ds) locations of the (a) emergent log A, (b) submerged log B, and (c) the reference point. Lower  $\zeta$  corresponds to less and higher  $\zeta$  to more pronounced clogging.

Table 7

Amount of declogging  $\Delta\zeta$  calculated with Equation (6). Positive  $\Delta\zeta$  indicates a decrease and negative values an increase in clogging.

Location	$\Delta\zeta(-)$	$\Delta z(m)$	$nABP(II\text{DOC})$ (mg/L)	$nABP(k_r)$ (m/s)	$\Delta FSF(\%)$	$\Delta\eta(-)$	$\Delta\varphi(-)$
A-us	0.069	0.20	6.3	3.4E-4	-7.80	0.017	5.29
A-ds	0.012	0.02	-0.5	-1.0E-5	-4.36	0.008	0.88
B-us	0.017	0.10	1.3	8.1E-4	0.14	0.012	-1.20
B-ds	0.026	0.03	0.2	-6.8E-4	1.53	-0.005	-3.96
Reference	-0.01	-0.07	0.1	n.a.	1.79	-0.01	-3.86

because of its small data requirements, which prohibits the use of data-driven models. Therefore, the here introduced fuzzy-logic method represents a suitable approach to leverage the combination of five clogging indicators into one representative indicator. In addition, the new in-

dicators  $\zeta$  and  $\Delta\zeta$  not only account for the trends of individual parameters that indicate clogging or declogging, but also their quantitative value. The membership functions make units that are otherwise non-comparable, such as percentages or mg/L, comparable in both their

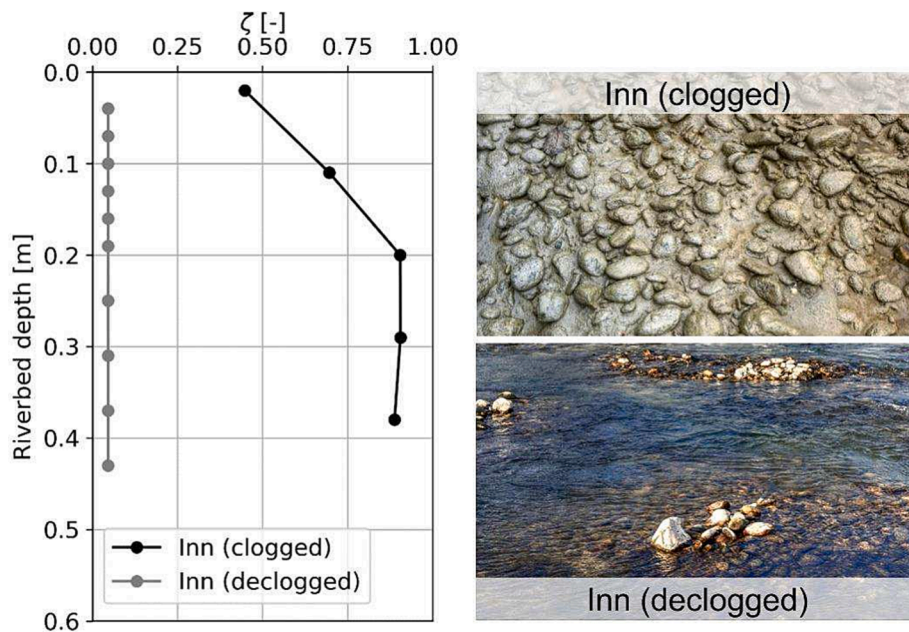


Fig. 9. The fuzzy degree of clogging at sites with clearly identifiable clogging state at the Inn River (Germany) with pictures featuring the clearly clogged (© IWS 2019) and declogged (© IWS 2020) measurement sites.

relative and absolute values. As a result, a holistic consideration of multiple individual clogging parameters with only a few records becomes possible through  $\zeta$  and  $\Delta\zeta$ .

The fuzzy indicators applied to the reference point insinuate that only flushing with high discharge and sediment addition is not sufficient to relief clogging. To confirm the validity of the indicators, the fuzzy inference system was additionally applied to de-facto clogged and declogged sites further upstream on the Inn River, where the degree of clogging  $\zeta$  was close to unity and zero, respectively (Fig. 9, detailed measurements and  $\zeta$  values are in the supplementary material). At one site, full clogging was concluded based on expert assessment of a gravel bar (Negreiros et al., 2023a), where the degree of clogging  $\zeta$  varied between 0.45 close to the surface and increased to 0.90 at a riverbed depth of 0.2 m. The lower (0.45) degree of clogging close to the surface can be attributed to still elevated yet invisible IDOC, while the riverbed was visually strongly clogged (Fig. 9). De-facto declogging was observed at a site where mechanical riverbed reshaping was performed with an excavator and fine sediment was washed out. Declogging with an excavator is only very locally effective, but not sustainable because it is a regularly needed intervention with heavy-duty machinery in sensitive aquatic ecosystems. The local short-term efficiency of the mechanically declogged site was characterized by  $\zeta = 0.05$  over the entire sampled riverbed depth (Fig. 9). While such clear expert statements regarding clogging are mostly not possible, the validity and representativeness of the fuzzy  $\zeta$  indicator could be confirmed at these two sites.

While fuzzy rules are transparent, replicable, and refer to crisp numbers, fuzzification is inherently vague due to intentionally imprecise boundaries (Klir and Wierman, 2013). In addition, other curve shapes, such as linear and threshold-based lines, are sometimes applied (Noack et al., 2013), but sigmoidal and parabolic functions are generally preferred for fuzzification because they are more representative (Garg, 2018; Garg and Ansha, 2018). This inherent vagueness of fuzzification means that a quantitative estimate for neither the truth of interpretations nor uncertainty cannot be calculated. Still, applied to a de-facto declogged sample and a visually strongly clogged sample (Fig. 9), the fuzzy approach proves a high degree of correct interpretation of clogging with low  $\zeta$  (i.e., a “low” degree of clogging) and high  $\zeta$  (i.e., a “high” degree of clogging) of the declogged and clogged samples, respectively. Therefore, also the assessment of declogging by  $\Delta\zeta$ , being the direct derivative of  $\zeta$ , can be considered relevant.

The fuzzy indicator of the degree of clogging  $\zeta$  can be considered as a robust quantity to express the state of riverbed clogging regarding variations in the input parameter values for fitting the membership functions. In particular, applied to the test case, the fuzzy inference system translated a 10% variation into an on-average 3.4% variation in  $\zeta$  (Fig. 8). However, the maximum  $\zeta$  uncertainty reached 10.4% in the vicinity of the steepest slopes of the fuzzy membership functions (Fig. 2), that is, the inflection points of the sigmoid functions (Equation (4)), determined by where their second derivative is zero (i.e., the  $b$ -values in Table 2). The MultiPAC points at log B caused the maximum  $\zeta$  uncertainty with their near-surface (0.12–0.15 m)  $FSF$  measurements. In general, the  $\zeta$  uncertainty upstream and downstream of log B was higher than at log A and the reference point, with similar uncertainty magnitudes before and after the flushing (Fig. 8). The generally higher uncertainty at log B originated from  $FSF$  measurements being close to the inflection point of the fuzzy membership functions for high  $FSF$ , which was at  $FSF = 14\%$  corresponding to the  $b$ -value of  $\mu_{high}$  in Table 2. In particular, the absolute maximum  $\zeta$  deviation from after the flushing corresponded to a measured  $FSF$  of 13.8%, and the percentage maximum  $\zeta$  deviation from before the flushing corresponded to a measured  $FSF$  of 13.7%. Thus, high-uncertainty regions of  $\zeta$  are where measurements are close to the inflection points of the fuzzy membership functions, but even then, the  $\zeta$  uncertainty is barely more than that of the input parameter values. The fuzzy indicators are therefore not only transferable to other sites, but also robust to uncertainties in the assumptions of

the fuzzy inference system.

Extending the fuzzy rule set to more parameters and parameter combinations would require more information to be available. For instance, the temperature of interstitial water is a known habitat parameter (Reeder et al., 2021; Thayaparan et al., 2019) and its vertical profile may provide additional information on vertical exchange processes. Also, the membership functions (Table 1) and fuzzy parameter combinations (Table 3) build on values reported in the literature or, where applicable, logic-based decision-making (see also supplementary material). However, not all parameter combinations could be accommodated based on available information. For example, Table 3 does not provide a rule for moderate clogging when  $FSF$  is high and IDOC is not low, which would be a refinement for the moderate clogging classification. Ideally, more rules would exist for more parameters, but based on the comprehensive literature review, the author’s best knowledge is that the required information is currently lacking.

#### 4.2. Parameter influence on the amount of declogging

Conflicting individual parameter indications may represent a problem for assessing the clogging status of a riverbed (Seitz, 2020). Typically, if three parameters indicate an increase in clogging and only one parameter indicates a decrease in clogging, the overall ecological condition regarding clogging would be subjectively considered to have worsened. While expert opinion might individually change, the amount of declogging  $\Delta\zeta$  does not, and it allows for the additional consideration of quantitative changes. For instance, downstream of the logs and at the reference point, the individual parameter changes were partially contradictory regarding clogging. In the wake of log A,  $nABP(IDOC)$  and  $nABP(k_f)$  indicated a slight increase in clogging, but the  $FSF$  decreased, and the porosity  $\eta$  and  $\varphi$  increased, suggesting declogging. However, neither  $\Delta\eta$ ,  $nABP(k_f)$ , nor  $\Delta\varphi$  was above the device precision downstream of log A, making their (de-)clogging trends irrelevant. Downstream of log B, the IDOC increased prominently ( $nABP(IDOC)$  of 0.2), indicating declogging, but the  $FSF$  increased, the  $k_f$  decreased ( $nABP(k_f) < 0$ ), and  $\varphi$  decreased, also at magnitudes above device precision, suggesting clogging. According to the fuzzy-based amount of declogging  $\Delta\zeta$ , the increase in  $nABP(IDOC)$  outweighed the ecologically disadvantageous evolution of the sum of the other parameters. Even though the sediment matrix was parametrically clogged, the hyporheic exchange downstream of log B was sufficient to cause little ecological concern, since oxygen levels are of primary importance for gravel-spawning fish (Ingendahl, 2001), and are related to permeable, declogged substrates. The reference point experienced slight coarsening, and a little increase in IDOC (Fig. 7c) suggested declogging, but the declogging trends were outweighed by a prominent increase in the  $FSF$  and a decrease in  $\varphi$  (Table 7).

The definition of the fuzzy inference system used to calculate the degree of clogging  $\zeta$  (Fig. 8) involves depth variability exclusively as a function of IDOC and  $k_f$ . While the  $k_f$  measurements were partially below the measurement precision level and could not be evaluated at the reference point after the flushing event, IDOC could always be measured with sufficient accuracy. Both IDOC and  $k_f$  profiles exhibited similar shapes, and their pronounced right shift after the flushing event was critical for the maximum amount of declogging  $\Delta\zeta$  to be located upstream of log A. This right shift can be attributed to fresh sediment deposits upstream of the logs, where declogging was clearly indicated by all parameters except for the bed-to-grain ratio  $\varphi$  at log B. Specifically, at log A, the decrease in  $\zeta$  can be related to a narrowly distributed, coarse, and 0.2 m thick sediment deposit that formed during the flushing event. The 0.1 m thick sediment deposit upstream of log B was also associated with a general, but weaker, declogging trend due to finer grain size compositions ( $D_{10}$  and  $FSF$ ).

Additionally, parameter weights can be introduced to give more importance to a specific clogging factor. For instance, if IDOC is of

primary interest to assess the effect of clogging on the oxygen availability for spawning redds of fish, steeper membership functions can be defined (i.e., values from Table 1 applied to Equation (4)).

While  $\Delta\zeta$  concluded a considerable ecological improvement upstream of log A, the improvements downstream of log A and in the surroundings of log B were only slightly apparent. These observations are consistent with the expectation that LW placement leads to locally increased bed disturbances and augmented hyporheic exchange (Doughty et al., 2020; Sawyer et al., 2012, 2011; Tonina and Buffington, 2007), but further research will be needed to optimize its declogging effects.

#### 4.3. Declogging potential of log placements

To avoid the regular need for mechanical interventions such as riverbed reshaping, this study tested LW placements in addition to a flushing event with the goal to yield sustainable declogging, which was partially efficient. In particular, declogging was prominent upstream of the baseflow-emergent log A, and the amount of declogging  $\Delta\zeta$  was generally higher in the vicinity of the LW placements (Table 7) than at the reference point. The negative  $\Delta\zeta$  at the reference point indicated that more clogging was present after the flushing event than before, which is the opposite of the declogging intended by the flushing event, and may be caused by fine sediment deposition during the falling limb of the flood. The positive topographic changes (i.e., deposition, cf. Table 7) upstream and downstream of the logs correspond to typical sediment trapping generated by LW (Poelman et al., 2019). Scour pools (see supplementary material) developed at the tips of the logs and were part of topographic patterns typical for large roughness elements at river banks, such as short, deflecting groins (Ishigaki and Baba, 2004). The deposition and scour patterns generated by LW turbulences can be expected to dynamically sustain in the future, that is, to self-renew because of the active sediment management of the fish pass (see experimental design). The deep scour pools and sediment deposits in the LW-typical local backwater of the logs (Follett et al., 2020) made these natural construction elements have similar effects on flushing hydrodynamics as technically engineered structures. In addition, the scouring at the log tips likely coarsened the sediment matrix by removing the fine sediment fraction (Bunte and Abt, 2001). However, we could not calculate the degree of declogging in the scour pools with MultiPAC measurements due to MultiPAC's application limits to wadeable water depths only. Nonetheless, scour pools in the vicinity of LW and their self-maintenance reportedly increase the abundance of fish and improve physical habitat quality for gravel-spawning fish (Brooks et al., 2004; Cederholm et al., 1997). In particular, the logs caused more bed disturbance than observed at the reference point, consistently with the intended, typical LW-induced increase in hydrodynamic variation (Follett et al., 2020; Schalko et al., 2021).

The emergent log A was associated with deposits of larger grain sizes, a considerable reduction in  $FSF$   $s$ , and an increase in porosity  $\eta$  after the flushing event. Even though log A was also submerged during the flushing event, its smaller submergence supposedly led to a decrease in parameters describing riverbed clogging. These changes could not be confirmed at the submerged log B. This observation is consistent with flume experiments showing that an emergent log has a more pronounced local hydro-geomorphic footprint than a submerged log with a less intense but larger footprint (Schalko et al., 2021).

The above discussion highlighted that the new fuzzy logic indicators  $\zeta$  and  $\Delta\zeta$  are robust and align with the parametric observations, indicating clogging improvement especially upstream of the baseflow-emergent log A. The  $\Delta\zeta$  values near the LW placements suggest an improvement in clogging that was not observed at the reference point. Therefore, the crisp parameter observations and fuzzy logic indicators provide evidence for not rejecting the hypothesis that an LW placement promotes declogging. Driven by large improvements in  $nABP$ (IDOC) and  $\Delta FSF$  (Table 5 and Table 7), the fuzzy-logic indicators point to

declogging downstream of log B, despite other MultiPAC parameters and subjective assessments potentially suggesting an increase in clogging. This contradiction illustrates the potential for the fuzzy-logic method to provide an objectively weighted and mathematically transparent assessment of riverbed clogging. In addition, the fuzzy inference system applied to all measurement points equally without the risk of statistical noise that could be caused when different experts judge the same sample (Kahneman et al., 2021). Thus, the novel fuzzy-logic method is a promising step toward a robust, objective assessment system, and LW placement showed encouraging effects to alleviate riverbed clogging.

## 5. Conclusions

A novel fuzzy-logic method has been developed to objectively and holistically measure the degree of riverbed clogging, taking into account five individual, physical substrate parameters. This method introduces new fuzzy-logic indicators to evaluate the effectiveness of declogging actions, allowing for an intuitive and objective assessment of stream restoration. It reduces subjectivity by excluding the statistical noise of expert assessment. The fuzzy-logic indicators contradicted subjective perceptions at one measurement point, as the novel fuzzy-logic method considers the resulting magnitude of measured parameters to describe declogging instead of relying on an expert comparison. Specifically, the fuzzy-logic method allows for quantitative scaling and thus objective comparison of the magnitude of measured parameters with different units. Thus, the new fuzzy-logic method represents a fundamental step toward objectifying the assessment of clogging.

To investigate the effect of large wood (LW) placements on riverbed clogging, the fuzzy-logic method was applied before and after a morphologically effective discharge. The fuzzy-logic indicators and individual parameter assessments showed that declogging occurred in the vicinity of LW placements while clogging occurred at a reference point far upstream without LW influence. This finding suggests that the hydro-morphological patterns generated by LW contribute to declogging, making LW placement a potentially effective tool for river restoration aimed at sustainable local declogging.

### Declaration of Competing Interest

The authors declare that they have no known competing financial interests or personal relationships that could have appeared to influence the work reported in this paper.

### Data availability

We provide all data and codes as described in the Acknowledgements and the code repositories cited in Negreiros et al. (2023b) and Schwindt et al. (2023).

### Acknowledgements

This work is the result of research collaboration supported by the MISTI Global Seed Funds MIT-Germany project (<https://misti.mit.edu/mit-germany>).

The authors gratefully acknowledge the invaluable contributions of Prof. Heidi Nepf, whose continuous mentorship has been critical to the realization of this research. Heidi Nepf's support in securing funding, assembling the author team, and constructive discussions to refine the analytical framework for assessing the impact of large wood on riverbed clogging greatly improved the implementation and robustness of this study.

Stefan Haun is indebted to the Baden-Württemberg Stiftung for the financial support of the Elite program for Postdocs. Isabella Schalko is funded by the Swiss National Science Foundation (Grant No. 209091).

The codes and data for calculating the degree of declogging were

implemented in the flusstools Python package (Negreiros et al., 2023b; Schwindt et al., 2023) along with this manuscript. Installation and usage instructions developed in this study are available at <https://flusstools.readthedocs.io> (BedAnalyst section).

The authors also are grateful to Verbund AG and the engineering firm ezB-fluss (Austria) for placing the logs and running the flushing experiment. In particular, we thank Rene Tezzele and his on-site dredger operators (Verbund AG), and Wolfgang Lauber (ezB) for their friendly and helpful cooperation.

The authors thank the efficient field team, including Maximilian Kunz, Gerhard Schmid, and Akash Handique, for the relentless work in all weather conditions, whether it was raining, storming, or snowing.

The authors also thank three anonymous reviewers whose productive comments led to substantial improvement of this work.

## Appendix A. Supplementary data

Supplementary data to this article can be found online at <https://doi.org/10.1016/j.ecolind.2023.111045>.

## References

- Acreman, M., Arthington, A.H., Colloff, M.J., Couch, C., Crossman, N.D., Dyer, F., Overton, I., Pollino, C.A., Stewardson, M.J., Young, W., 2014. Environmental flows for natural, hybrid, and novel riverine ecosystems in a changing world. *Frontiers in Ecology and the Environment* 12, 466–473. <https://doi.org/10.1890/130134>.
- Albert, C., Hack, J., Schmidt, S., Schröter, B., 2021. Planning and governing nature-based solutions in river landscapes: Concepts, cases, and insights. *Ambio* 50, 1405–1413. <https://doi.org/10.1007/s13280-021-01569-z>.
- Allan, D.J., Castillo, M.M., 2007. *Stream ecology - structure and function of running waters*, Second. ed. Springer, Dordrecht, The Netherlands.
- Battin, T.J., Sengschmitt, D., 1999. Linking sediment biofilms, hydrodynamics, and river bed clogging: Evidence from a large river. *Microbial Ecology* 37, 185–196.
- Blaschke, A.P., Steiner, K.-H., Schmalfluss, R., Gutknecht, D., Sengschmitt, D., 2003. Clogging processes in hyporheic interstices of an impounded river, the danube at vienna, austria. *International Review of Hydrobiology* 88, 397–413.
- Boulton, A.J., 2007. Hyporheic rehabilitation in rivers: restoring vertical connectivity. *Freshwater Biology* 52, 632–650. <https://doi.org/10.1111/j.1365-2427.2006.01710.x>.
- Bouwer, H., 1966. Rapid field measurement of air entry value and hydraulic conductivity of soil as significant parameters in flow system analysis. *Water Resources Research* 2, 729–738. <https://doi.org/10.1029/WR002i004p00729>.
- Brooks, A.P., Gehrke, P.C., Jansen, J.D., Abbe, T.B., 2004. Experimental reintroduction of woody debris on the williams river, NSW: Geomorphic and ecological responses. *River Research and Applications* 20, 513–536. <https://doi.org/10.1002/rra.764>.
- Brunke, M., Gonser, T., 1997. The ecological significance of exchange processes between rivers and groundwater. *Freshwater Biology* 37, 1–33. <https://doi.org/10.1046/j.1365-2427.1997.00143.x>.
- Bunte, K., 2004. *Gravel mitigation and augmentation below hydroelectric dams: A geomorphological perspective*. Colorado State University, Fort Collins, CO, USA, Engineering Research Center.
- Bunte, K., Abt, S.R., 2001. *Sampling Surface and Subsurface Particle-Size Distributions in Wadable Gravel- and Cobble-Bed Streams for Analyses in Sediment Transport, Hydraulics, and Streambed Monitoring (General Technical, No. RMRS-GTR-74)*. United States Department of Agriculture, Fort Collins, CO, USA.
- Carling, P.A., Reader, N.A., 1981. A freeze-sampling technique suitable for coarse river bed-material. *Sedimentary Geology* 29, 233–239. [https://doi.org/10.1016/0037-0738\(81\)90009-9](https://doi.org/10.1016/0037-0738(81)90009-9).
- Cederholm, C.J., Bilby, R.E., Bisson, P.A., Bumstead, T.W., Fransen, B.R., Scarlett, W.J., Ward, J.W., 1997. Response of juvenile coho salmon and steelhead to placement of large woody debris in a coastal washington stream. *North American Journal of Fisheries Management* 17, 947–963. [https://doi.org/10.1577/1548-8675\(1997\)017<0947:ROJCSA>2.3.CO;2](https://doi.org/10.1577/1548-8675(1997)017<0947:ROJCSA>2.3.CO;2).
- Chapman, D.W., 1988. *Critical review of variables used to define effects of fines in redds of large salmonids*. *Transactions of the American Fisheries Society* 117, 1–21.
- Cunningham, A.B., Anderson, C.J., Bouwer, H., 1987. Effects of Sediment-Laden flow on channel bed clogging. *Journal of Irrigation and Drainage Engineering* 113, 106–118. [https://doi.org/10.1061/\(ASCE\)0733-9437\(1987\)113:1\(106\)](https://doi.org/10.1061/(ASCE)0733-9437(1987)113:1(106)).
- Datry, T., Lamouroux, N., Thivin, G., Descloux, S., Baudoin, J.M., 2015. Estimation of sediment hydraulic conductivity in river reaches and its potential use to evaluate streambed clogging. *river Research and Applications* 31, 880–891. <https://doi.org/10.1002/rra.2784>.
- de Oliveira, J., 1995. A set-theoretical defuzzification method. *Fuzzy Sets and Systems* 76, 63–71. [https://doi.org/10.1016/0165-0114\(95\)00002-3](https://doi.org/10.1016/0165-0114(95)00002-3).
- Descloux, S., Datry, T., Philippe, M., Marmonier, P., 2010. Comparison of different techniques to assess surface and subsurface streambed colmatation with fine sediments. *International Review of Hydrobiology* 95, 520–540. <https://doi.org/10.1002/iroh.201011250>.
- Doughty, M., Sawyer, A.H., Wohl, E., Singha, K., 2020. Mapping increases in hyporheic exchange from channel-spanning logjams. *Journal of Hydrology* 587, 124931. <https://doi.org/10.1016/j.jhydrol.2020.124931>.
- Dubuis, R., De Cesare, G., 2023. The clogging of riverbeds: A review of The physical processes. *Earth-Science Reviews* 239, 104374. <https://doi.org/10.1016/j.earscirev.2023.104374>.
- Duch, W., 2005. Uncertainty of data, fuzzy membership functions, and multilayer perceptrons. *IEEE Transactions on Neural Networks* 16, 10–23. <https://doi.org/10.1109/TNN.2004.836200>.
- Einstein, H.A., 1968. Deposition of suspended particles in a gravel bed. *Journal of the Hydraulics Division* 94, 1197–1206.
- Einstein, H.A., 1970. Closure to “Deposition of suspended particles in a gravel bed”. *Journal of the Hydraulics Division* 96, 581–582. <https://doi.org/10.1061/JYCEAJ.0002353>.
- Eriksen, C.H., 1968. Ecological significance of respiration and substrate for burrowing ephemeroptera. *Canadian Journal of Zoology* 46, 93–103. <https://doi.org/10.1139/z68-015>.
- Fausch, K.D., 1993. Experimental analysis of microhabitat selection by juvenile steelhead (*Oncorhynchus mykiss*) and coho salmon (*O. kisutch*) in a british columbia stream. *Canadian Journal of Fisheries and Aquatic Sciences* 50, 1198–1207. <https://doi.org/10.1139/f93-136>.
- Fletcher, W.K., McLean, W.E., Sweeten, T., 1995. An instrument to monitor infiltration of fine sediment into stable gravel stream beds. *Aquacultural Engineering* 14, 289–296. [https://doi.org/10.1016/0144-8609\(94\)00007-N](https://doi.org/10.1016/0144-8609(94)00007-N).
- Follett, E., Schalko, I., Nepf, H., 2020. Momentum and energy predict the backwater rise generated by a large wood jam. *Geophysical Research Letters* 47.
- Franssen, J., Lapointe, M., Magnan, P., 2014. Geomorphic controls on fine sediment re-infiltration into salmonid spawning gravels and the implications for spawning habitat rehabilitation. *Geomorphology* 211, 11–21. <https://doi.org/10.1016/j.geomorph.2013.12.019>.
- Frings, R.M., Schüttrumpf, H., Vollmer, S., 2011. Verification of porosity predictors for fluvial sand-gravel deposits. *Water Resources Research* 47. <https://doi.org/10.1029/2010WR009690>.
- Garg, H., 2018. Some arithmetic operations on the generalized sigmoidal fuzzy numbers and its application. *Granul. Comput.* 3, 9–25. <https://doi.org/10.1007/s41066-017-0052-7>.
- Garg, H., Ansha, 2018. Arithmetic Operations on Generalized Parabolic Fuzzy Numbers and Its Application. *Proc. Natl. Acad. Sci., India, Sect. A Phys. Sci.* 88, 15–26. <https://doi.org/10.1007/s40010-016-0278-9>.
- Gibson, R.J., 1993. The atlantic salmon in fresh water: spawning, rearing and production. *Reviews in Fish Biology and Fisheries* 3, 39–73. <https://doi.org/10.1007/BF00043297>.
- Gibson, S., Abraham, D., Heath, R., Schoellhamer, D., 2009. Vertical gradational variability of fines deposited in a gravel framework. *Sedimentology* 56, 661–676. <https://doi.org/10.1111/j.1365-3091.2008.00991.x>.
- Grabowski, R.C., Gurnell, A.M., Burgess-Gamble, L., England, J., Holland, D., Klaar, M.J., Morrissey, I., Uttley, C., Wharton, G., 2019. The current state of The use of large wood in river restoration and management. *Water and Environment Journal* 33, 366–377. <https://doi.org/10.1111/wej.12465>.
- Grygoruk, M., Szaikiewicz, E., Grodzka-Lukaszewska, M., Mirosław-Świątek, D., Ogłęcki, P., Pustowska-Tyszewska, D., Sinicyn, G., Okruszko, T., 2021. Revealing the influence of hyporheic water exchange on the composition and abundance of bottom-dwelling macroinvertebrates in a temperate lowland river. *Knowledge and Management of Aquatic Ecosystems* 37. <https://doi.org/10.1051/kmae/2021036>.
- Harbaugh, A.W., 2005. *MODFLOW-2005, The U.S. Geological Survey Modular Ground-Water Model – the Ground-Water Flow Process (techreport No. USGS TM 6-A16)*, U. S. Geological Survey Techniques and Methods. U.S. Department of the Interior, U.S. Geological Survey, Reston, VA, USA.
- Harper, S.E., Foster, I.D.L., Lawler, D.M., Mathers, K. I., McKenzie, M., Petts, G.E., 2017. The complexities of measuring fine sediment accumulation within gravel-bed rivers. *River Research and Applications* 33, 1575–1584. <https://doi.org/10.1002/rra.3198>.
- Harrison, L.R., Legleiter, C.J., Wydzga, M.A., Dunne, T., 2011. Channel dynamics and habitat development in a meandering, gravel bed river. *Water Resources Research* 47, W04513. <https://doi.org/10.1029/2009WR008926>.
- Harrison, L.R., Bray, E., Overstreet, B., Legleiter, C.J., Brown, R.A., Merz, J.E., Bond, R. M., Nicol, C.L., Dunne, T., 2019. Physical controls on salmon redd site selection in restored reaches of a regulated, Gravel-Bed river. *Water Resources Research* 55, 8942–8966. <https://doi.org/10.1029/2018WR024428>.
- Harrod, T.R., Theurer, F.D., 2002. *Sediment*, in: *Agriculture, Hydrology, and Water Quality*. CABI Pub., Wallingford, UK; New York, pp. 155–170.
- Haun, S., Negreiros, B., Kunz, M., Schwindt, S., Galdos, A.A., Noack, M., Wiprecht, S., 2022. MultiPAC: A novel approach to quantify the clogging degree of a riverbed (No. EGU22-1318). Presented at the EGU22, Copernicus Meetings. <https://doi.org/10.5194/egusphere-egu22-1318>.
- Heywood, M.J.T., Walling, D.E., 2007. The sedimentation of salmonid spawning gravels in The hampshire avon catchment, UK: implications for The dissolved oxygen content of intragravel water and embryo survival. *Hydrological Processes* 21, 770–788. <https://doi.org/10.1002/hyp.6266>.
- Huston, D.L., Fox, J.F., 2015. Clogging of fine sediment within gravel substrates: Dimensional analysis and macroanalysis of experiments in hydraulic flumes. *Journal of hydraulic Engineering* 141, 04015015. [https://doi.org/10.1061/\(ASCE\)HY.1943-7900.0001015](https://doi.org/10.1061/(ASCE)HY.1943-7900.0001015).
- Ingendahl, D., 2001. Dissolved oxygen concentration and emergence of sea trout fry from natural redds in tributaries of the river rhine. *Journal of Fish Biology* 58, 325–341. <https://doi.org/10.1111/j.1095-8649.2001.tb02256.x>.

- Ishigaki, T., Baba, Y., 2004. Local Scour Induced By 3D Flow Around Attracting And Deflecting Groins, in: Proceedings 2nd International Conference on Scour and Erosion (ICSE-2). November 14-17, 2004. Presented at the 2nd International Conference on Scour and Erosion (ICSE-2), Singapore, p. 8.
- Jones, J.L., Murphy, J.F., Collins, A.L., Sear, D.A., Naden, P.S., Armitage, P.D., 2012. The impact of fine sediment On Macro-Invertebrates. *River Research and Applications* 28, 1055–1071. <https://doi.org/10.1002/rra.1516>.
- Kahneman, D., Sibony, O., Sunstein, C.R., 2021. *Noise: a flaw in human judgment, first edition*. ed. Harper Collins Publishers, New York, NY, USA, William Collins.
- Keller, E.A., Swanson, F.J., 1979. Effects of large organic material on channel form and fluvial processes. *Earth Surface Processes* 4, 361–380. <https://doi.org/10.1002/esp.3290040406>.
- Klir, G., Wierman, M.J., 2013. *Uncertainty-based information: Elements of generalized information theory (studies in fuzziness and soft computing)*, 2nd ed. Physica-Verlag, Heidelberg, Germany.
- Latorre, B., Moret-Fernández, D., Peña, C., 2013. Estimate of soil hydraulic properties from disc infiltrometer three-dimensional infiltration curve: Theoretical analysis and field applicability. *Procedia Environmental Sciences, Four Decades of Progress in Monitoring and Modeling of Processes in the soil-Plant-Atmosphere System: Applications and Challenges* 19, 580–589. <https://doi.org/10.1016/j.proenv.2013.06.066>.
- Leopold, L.B., Wolman, M.G., 1957. River Channel Patterns: Braided, Meandering and Straight. USGS professional paper 282-B, 1–85.
- Lindroth, A., 1942. Sauerstoffverbrauch der fische. II. Verschiedene entwicklungs- und alterstadien vom lachs und hecht [Oxygen consumption by fish. II. different development and age stages of salmon and pike]. *Z. Vergl. Physiol.* 29, 583–594. <https://doi.org/10.1007/BF00304682>.
- Lisle, T.E., 1989. Sediment transport and resulting deposition in spawning gravels, north coastal California. *Water Resources Research* 25, 1303–1319. <https://doi.org/10.1029/WR025i006p1303>.
- Maridet, L., Philippe, M., 1995. influence of substrate characteristics on the vertical distribution of stream macroinvertebrates in the hyporheic zone. *Biologia* 91, 101–105.
- Maridet, L., Wasson, J.-G., Philippe, M., 1992. Vertical distribution of fauna in the bed sediment of three running water sites: Influence of physical and trophic factors. *Regulated Rivers: Research & Management* 7, 45–55. <https://doi.org/10.1002/rrr.3450070107>.
- Marmonier, P., Delettre, Y., Lefebvre, S., Guyon, J., Boulton, A.J., 2004. A simple technique using wooden stakes to estimate vertical patterns of interstitial oxygenation in the beds of rivers. *Archiv für Hydrobiologie* 133–143. <https://doi.org/10.1127/0003-9136/2004/0160-0133>.
- Mayar, M.A., Haun, S., Schmid, G., Wieprecht, S., Noack, M., 2022. Measuring vertical distribution and dynamic development of sediment infiltration under laboratory conditions. *Journal of Hydraulic Engineering* 148, 04022008. [https://doi.org/10.1061/\(ASCE\)HY.1943-7900.0001980](https://doi.org/10.1061/(ASCE)HY.1943-7900.0001980).
- Mohammadi, S.D., Nikoudeh, M.R., Rahimi, H., Khamsehchiyan, M., 2008. Application of the dynamic cone penetrometer (DCP) for determination of the engineering parameters of sandy soils. *Engineering Geology* 101, 195–203. <https://doi.org/10.1016/j.enggeo.2008.05.006>.
- Moring, J.R., 1982. Decrease in stream gravel permeability after clear-cut logging: an indication of intragravel conditions for developing salmonid eggs and alevins. *Hydrobiologia* 88, 295–298. <https://doi.org/10.1007/BF00008510>.
- Nagel, C., Mueller, M., Pander, J., Geist, J., 2020. Making up the bed: Gravel cleaning as a contribution to nase (*Chondrostoma nasus* L.) spawning and recruitment success. *Aquatic Conservation: Marine and Freshwater Ecosystems* 30, 2269–2283. <https://doi.org/10.1002/aqc.3458>.
- Negreiros, B., Barros, R., Schwindt, S., 2023b. BedAnalyst - a FlussTools package. <https://doi.org/10.17605/OSF.IO/G7K52>.
- Negreiros, B., Galdos, A.A., Seitz, L., Noack, M., Schwindt, S., Wieprecht, S., Haun, S., 2023a. A multi-parameter approach to quantify riverbed clogging and natural hyporheic connectivity. *River Research and Applications* n/a 1–8. <https://doi.org/10.1002/rra.4145>.
- Noack, M., Schneider, M., Wieprecht, S., 2013. Ecohydraulics: an integrated approach, in: Maddock, I., Harby, A., Kemp, P., Wood, P. (Eds.), Wiley-Blackwell, Chichester, UK, pp. 75–91.
- Packman, A.L., Salehin, M., Zaramella, M., 2004. Hyporheic exchange with gravel beds: Basic hydrodynamic interactions and Bedform-Induced advective flows. *Journal of Hydraulic Engineering* 130, 647–656. [https://doi.org/10.1061/\(ASCE\)0733-9429\(2004\)130:7\(647\)](https://doi.org/10.1061/(ASCE)0733-9429(2004)130:7(647)).
- Pasternack, G.B., Wyrick, J.R., 2017. Flood-driven topographic changes in a gravel-cobble river over segment, reach, and morphological unit scales. *Earth Surface Processes and Landforms* 42, 487–502. <https://doi.org/10.1002/esp.4064>.
- Pasternack, G.B., 2020. River Restoration: Disappointing, Nascent, Yet Desperately Needed\*, in: Reference Module in Earth Systems and Environmental Sciences. Elsevier. <https://doi.org/10.1016/B978-0-12-409548-9.12449-2>.
- Patro, S.G.K., Sahu, K.K., 2015. Normalization: A Preprocessing Stage. <https://doi.org/10.48550/arXiv.1503.06462>.
- Petts, G.E., Thoms, M.C., Brittan, K., Atkin, B., 1989. A freeze-coring technique applied to pollution by fine sediments in gravel-bed rivers. *Science of The Total Environment* 84, 259–272. [https://doi.org/10.1016/0048-9697\(89\)90388-4](https://doi.org/10.1016/0048-9697(89)90388-4).
- Poelman, J.Y., Hoitink, A.J.F., de Ruijscher, T.V., 2019. Flow and bed morphology response to the introduction of wood logs for sediment management. *Advances in Water Resources* 130, 1–11. <https://doi.org/10.1016/j.advwatres.2019.05.023>.
- Reeder, W.J., Gariglio, F., Carnie, R., Tang, C., Isaak, D., Chen, Q., Yu, Z., McKean, J.A., Tonina, D., 2021. Some (fish might) like it hot: Habitat quality and fish growth from past to future climates. *Science of The Total Environment* 787, 147532. <https://doi.org/10.1016/j.scitotenv.2021.147532>.
- Reiser, D.W., White, R.G., 1988. Effects of two sediment Size-Classes on survival of steelhead and chinook salmon eggs. *North American Journal of Fisheries Management* 8, 432–437. [https://doi.org/10.1577/1548-8675\(1988\)008<0432: EOTSSC>2.3.CO;2](https://doi.org/10.1577/1548-8675(1988)008<0432: EOTSSC>2.3.CO;2).
- Rezaee, M.R., Kadkhodaie-Ilkhchi, A., Alizadeh, P.M., 2008. Intelligent approaches for the synthesis of petrophysical logs. *Journal of Geophysics and Engineering* 5, 12–26. <https://doi.org/10.1088/1742-2132/5/1/002>.
- Roni, P., Beechie, T., Pess, G., Hanson, K., 2015. Wood placement in river restoration: fact, fiction, and future direction. *Canadian Journal of Fisheries and Aquatic Sciences* 72, 466–478. <https://doi.org/10.1139/cjfas-2014-0344>.
- Rubin, J.-F., 1998. Survival and emergence pattern of sea trout fry in substrata of different compositions. *Journal of Fish Biology* 53, 84–92. <https://doi.org/10.1111/j.1095-8649.1998.tb00111.x>.
- Rubin, J.-F., Glimsäter, C., 1996. Egg-to-fry survival of the sea trout in some streams of gotland. *Journal of Fish Biology* 48, 585–606. <https://doi.org/10.1111/j.1095-8649.1996.tb01454.x>.
- Sawyer, A.H., Bayani Cardenas, M., Buttles, J., 2011. Hyporheic exchange due to channel-spanning logs. *Water Resources Research* 47. <https://doi.org/10.1029/2011WR010484>.
- Sawyer, A.H., Bayani Cardenas, M., Buttles, J., 2012. Hyporheic temperature dynamics and heat exchange near channel-spanning logs. *Water Resources Research* 48. <https://doi.org/10.1029/2011WR011200>.
- Sawyer, A.M., Pasternack, G.B., Moir, H.J., Fulton, A.A., 2010. Riffle-pool maintenance and flow convergence routing observed on a large gravel-bed river. *Geomorphology* 114, 143–160. <https://doi.org/10.1016/j.geomorph.2009.06.021>.
- Schaelchli, A., 2002. Kolmation. Eawag, Duebendorf/Zurich, Switzerland, Methoden zur Erkennung und Bewertung (Schlussbericht).
- Schälchli, U., 1992. The clogging of coarse gravel river beds by fine sediment. *Hydrobiologia* 235, 189–197. <https://doi.org/10.1007/BF00026211>.
- Schalko, I., Wohl, E., Nepf, H.M., 2021. Flow and wake characteristics associated with large wood to inform river restoration. *Scientific Reports* 11, 8644. <https://doi.org/10.1038/s41598-021-87892-7>.
- Schwindt, S., Negreiros, B., Barros, R., Henning, N., Mouris, K., 2023. FlussTools. <https://doi.org/10.17605/OSF.IO/G7K52>.
- Seitz, L., 2020. Development of new methods to apply a multi-parameter approach – A first step towards the determination of colmation (phdthesis). University of Stuttgart, Stuttgart, Germany.
- Sennatt, K.M., Salant, N.L., Renshaw, C.E., Magilligan, F.J., 2006. Assessment of methods for measuring embeddedness: Application to sedimentation in flow regulated Streams1. *JAWRA Journal of the American Water Resources Association* 42, 1671–1682. <https://doi.org/10.1111/j.1752-1688.2006.tb06028.x>.
- Senter, A.E., Pasternack, G.B., 2011. Large wood aids spawning chinook salmon (*Oncorhynchus tshawytscha*) in marginal habitat on a regulated river in California. *River Research and Applications* 27, 550–565. <https://doi.org/10.1002/rra.1388>.
- Smith, D.L., Goodwin, R.A., Nestler, J.M., 2014. Relating turbulence and fish habitat: A new approach for management and research. *Reviews in Fisheries Science & Aquaculture* 22, 123–130. <https://doi.org/10.1080/10641262.2013.803516>.
- Sowden, T.K., Power, G., 1985. Prediction of rainbow trout embryo survival in relation to groundwater seepage and particle size of spawning substrates. *Transactions of the American Fisheries Society* 114, 804–812. [https://doi.org/10.1577/1548-8659\(1985\)114<804:PORTES>2.0.CO;2](https://doi.org/10.1577/1548-8659(1985)114<804:PORTES>2.0.CO;2).
- Thayaparan, A., Syed, F., Liang, L., Dodge, N., 2019. Dissolved oxygen and temperature on the viability of spawning salmon. *The Expedition* 9.
- Tonina, D., Buffington, J.M., 2007. Hyporheic exchange in gravel bed rivers with pool-riffle morphology: Laboratory experiments and three-dimensional modeling. *Water Resources Research* 43. <https://doi.org/10.1029/2005WR004328>.
- Tullos, D., Walter, C., 2015. Fish use of turbulence around wood in winter: physical experiments on hydraulic variability and habitat selection by juvenile coho salmon, *oncorhynchus kisutch*. *Environ Biol Fish* 98, 1339–1353. <https://doi.org/10.1007/s10641-014-0362-4>.
- Ulrich, C., Hubbard, S.S., Florsheim, J., Rosenberry, D., Borglin, S., Trotta, M., Seymour, D., 2015. Riverbed clogging associated with a California riverbank filtration system: An assessment of mechanisms and monitoring approaches. *Journal of Hydrology* 529, 1740–1753. <https://doi.org/10.1016/j.jhydrol.2015.08.012>.
- Ward, J.C., 1964. Turbulent flow in porous media. *Journal of the Hydraulics Division* 90, 1–12. <https://doi.org/10.1061/JYCEAJ.0001096>.
- Wharton, G., Mohajeri, S.H., Righetti, M., 2017. The pernicious problem of streambed colmation: a multi-disciplinary reflection on The mechanisms, causes, impacts, and management challenges. *WIREs Water* 4, e1231.
- Wickett, W.P., 1954. The oxygen supply to salmon eggs in spawning beds. *J. Fish. Res. Bd. Can.* 11, 933–953. <https://doi.org/10.1139/f54-053>.
- Wohl, E., Lane, S.N., Wilcox, A.C., 2015. The science and practice of river restoration. *Water Resources Research* 51, 5974–5997. <https://doi.org/10.1002/2014WR016874>.
- Wolman, M.G., Leopold, L.B., 1957. River flood plains some observations on their formation. Physiographic and hydraulic studies of rivers. Geological Survey Professional Paper 282-C, 1–107.
- Wolman, M.G., Miller, J.P., 1960. Magnitude and frequency of forces in geomorphic processes. *The Journal of Geology* 68, 54–74.
- Wood, P.J., Armitage, P.D., 1997. Biological effects of fine sediment in the lotic environment. *environmental Management* 21, 203–217.
- Woodworth, K.A., Pasternack, G.B., 2022. Are dynamic fluvial morphological unit assemblages statistically stationary through floods of less than ten times bankfull

- discharge? *Geomorphology* 403, 108135. <https://doi.org/10.1016/j.geomorph.2022.108135>.
- Wooster, J.K., Dusterhoff, S.R., Cui, Y., Sklar, L.S., Dietrich, W.E., Malko, M., 2008. Sediment supply and relative size distribution effects on fine Sediment infiltration into immobile gravels. *Water Resources Research* 44.
- Zadeh, L.A., 1965. Fuzzy sets. *Information and Control* 8, 338–353. [https://doi.org/10.1016/S0019-9958\(65\)90241-X](https://doi.org/10.1016/S0019-9958(65)90241-X).
- Zauner, G., Lauber, W., Jung, M., Ratschan, C., Schöfbenker, M., Schmalfuß, R., 2020. Wie erreicht man das „gute ökologische Potenzial“? Fallbeispiel Innstauraum Eggfling-Obernberg. *Österr Wasser- und Abfallw.* <https://doi.org/10.1007/s00506-020-00672-x>.
- Zumbroich, T., Hahn, H.-J., 2018. Feinsedimenteinträge in Gewässern und deren Messung - Kolmation als bedeutsamer Störfaktor bei der Umsetzung der EG-WRRL [Fine sediment inputs to water bodies and their measurement - riverbed clogging as a significant disturbance factor in the implementation of the EC-WFD], in: M3-Messen, Modellieren, Managen in Hydrologie Und Wasserressourcenbewirtschaftung. Presented at the Forum fuer Hydrologie und Wasserbewirtschaftung, DWA, Dresden, Germany, pp. 193–202. <https://doi.org/10.14617/for.hydrol.wasbew.39.18>.